

Synthesis and hyperpolarization of ^{13}C and ^2H labeled vinyl pyruvate and pyruvate

Arne Brahms^{[a]†*}, Andrey N. Pravdivtsev^{[b]†*}, Tim Stamp^[a], Frowin Ellermann^[b], Frank D. Sönnichsen^[a], Jan-Bernd Hövener^{[b] ‡}, Rainer Herges^{[a]†*}

[a] A. Brahms, T. Stamp, Prof. Dr. F. Sönnichsen, Prof. Dr. R. Herges
Otto Diels Institute for Organic Chemistry, Kiel University
Kiel University, Otto- Hahn Platz 4, 24118 Kiel, Germany
E-mail: abrahms@oc.uni-kiel.de, rherges@oc.uni-kiel.de

[b] Dr. A. N. Pravdivtsev, Prof. Dr. J.-B. Hövener, F. Ellermann
Section Biomedical Imaging, Molecular Imaging North Competence Center (MOIN CC)
Department of Radiology and Neuroradiology, University Medical Center Kiel
Kiel University, Am Botanischen Garten 14, 24118, Kiel, Germany
E-mail: andrey.pravdivtsev@rad.uni-kiel.de, jan.hoevener@rad.uni-kiel.de

Keywords: hyperpolarization • ketocarboxylic acid • parahydrogen • vinyl ester • vinyl pyruvate •

†,‡ these authors contributed equally, * corresponding authors

Supporting information for this article is given via a link at the end of the document (wanst sure if need we delete this)

Abstract: The hyperpolarization of nuclear spins has enabled unique applications in chemistry, biophysics, and particularly in metabolic imaging. Parahydrogen-induced polarization (PHIP) offers a fast and cost-efficient way of hyperpolarization. Nevertheless, PHIP lags behind dynamic nuclear polarization (DNP), which is already being evaluated in clinical studies. This shortcoming is mainly due to problems in the synthesis of the corresponding PHIP precursor molecules. The most widely used DNP tracer in clinical studies, particularly for the detection of prostate cancer, is 1- ^{13}C -pyruvate. The ideal derivative for PHIP is the deuterated vinyl ester because the spin physics allows for 100% polarization. Unfortunately, there is no efficient synthesis for vinyl esters of β -ketocarboxylic acids in general and pyruvate in particular. Here, we present an efficient new method for the preparation of vinyl esters, including ^{13}C labeled, fully deuterated vinyl pyruvate using a palladium catalyzed procedure. Using 50 % enriched parahydrogen and mild reaction conditions, a ^{13}C polarization of 12% was readily achieved; 36% are expected with 100% pH_2 . Higher polarization values can be potentially achieved with optimized reaction conditions.

Introduction

Nuclear magnetic resonance (NMR) and magnetic resonance imaging (MRI) are among the most powerful analytical methods in chemistry, physics, and medicine.^[1-3] It is a well-known fact, however, that both methods exploit only a very small part of their actual potential. The sensitivity is of the order of a few parts per million due to the low spin polarization of the magnetically active nuclei. The need for more sensitive MR is addressed by hardware improvements that include the construction of systems with higher magnetic fields and the use of cryo-probes.^[4,5] These strategies, however, are expensive and limited by a sensitivity gain of one order of magnitude. Hyperpolarization (HP), on the other hand, is a more effective approach that allows to amplify the signal of selected molecules by a factor of 10^4 - 10^6 , surpassing any current hardware technology. This increase in sensitivity has opened up entirely new applications such as to visualize metabolic processes beyond the conventional anatomical MRI imaging. It is therefore not surprising that hyperpolarization has experienced a steep upswing within the last decade.

Nevertheless, there are still restrictions that prevent a general use of these methods.

Dynamic nuclear polarization (DNP)^[6,7] is the most elaborate HP method with applications from proteomics^[8] to real-time *in vivo* metabolomics.^[9,10] The rapid development of dissolution DNP (dDNP) was triggered by the discovery of fast *in vivo* conversion of hyperpolarized 1- ^{13}C -pyruvate (1- ^{13}C -Pyr) to 1- ^{13}C -lactate (1- ^{13}C -Lac) in some malignant tumors and inflammations, known as the Warburg effect.^[11] Administration of hyperpolarized 1- ^{13}C -Pyr and monitoring metabolic conversion by MRI *in vivo* is considered to be a promising modality to detect early stages of prostate and breast cancer.^[12] However, the main drawback of dDNP (disregard the high price) is its relatively low hyperpolarization throughput, which for commercial systems is ~1 hour per sample while the lifetime of HP 1- ^{13}C -pyruvate is only ~1 minute.

Parahydrogen-induced polarization (PHIP) is another quickly developing HP method.^[13,14] Here, the spin order of parahydrogen (pH_2) is used to enhance the MR signal of dedicated contrast agents. pH_2 and orthohydrogen (oH_2) are the

two nuclear magnetic spin isomers of H₂. pH₂ is a singlet state and asymmetric with respect to the exchange of two nuclear spins, while oH₂ is a triplet spin state and symmetric under nuclear spin exchange. Following the Boltzmann distribution, at room temperature, 75% of H₂ is in the ortho state, and 25% is pH₂. At 77K (liquid nitrogen), the pH₂ fraction is about 50%, and at 21K (boiling point of H₂), it is >99%. pH₂ can be produced in bulk and stored for days, making it a convenient and readily available source of nuclear spin order.^[15–17]

The spin order of pH₂ can be used to enhance the ¹³C^[18–21] or ¹⁵N^[22–24] magnetization of a contrast agent either by temporary contact (signal amplification by reversible exchange, SABRE)^[25] or by pairwise addition of pH₂ to an unsaturated precursor (catalytic hydrogenation).^[26] The fact that many biologically interesting compounds do not have an unsaturated precursor has long hindered the development of PHIP. This restriction, however, was mitigated by adding an unsaturated side group (unsaturated auxiliary group, UAG) to the desired contrast agents.^[27–29] After hydrogenation of the side group and polarization transfer to the main molecule, the auxiliary group was cleaved and the desired contrast agents resulted.

To date, mainly allyl-, propargyl- and vinyl esters have been used as side arms or “unsaturated auxiliary groups” (UAGs).^[30]

So far, 1-¹³C-Pyr or its precursors were polarized to a maximum value of 6.2% by a sidearm hydrogenation (PHIP-SAH) of allyl-pyruvate^[31,32] and 10.8% by SABRE.^[33] The practicability of the PHIP-SAH method was demonstrated in cells^[34] and animal models in vivo.^[31] However, the polarization yield is still lower for allyl or propargyl precursors than for vinyl precursors.

The transfer of pH₂-derived spin order into polarization of a third nucleus is most efficient if there are no other nuclei interacting with pH₂, or if the interactions can be canceled.^[21,35] In these cases, the spin system is effectively a three spin-½ system, and X-nuclei polarization of 100% can be achieved.

Such a spin system can be approximated by deuteration of all non-participating protons and selective labeling of the X-nuclei of choice (e.g. ¹³C or ¹⁵N). Vinyl esters are particularly suited as UAGs because desired three-spin system is easily realized if the vinyl group is fully deuterated (disregarding couplings of the ¹³C to other nuclei in the main molecule). Also important is that the added hydrogens are only 3 and 4 bonds away from the carbonyl ¹³C atom, which facilitates polarization transfer. This method has been applied to prepare ¹³C polarization levels exceeding 50% for ethyl acetate-*d*6 from fully deuterated vinyl acetate.^[21]

Encouraged by these results, we set out to synthesize 1-¹³C-vinyl-pyruvate-*d*6, which is the precursor of the probably most promising metabolic tracer for hyperpolarized MRI as mentioned earlier. After parahydrogenation of the vinyl group, followed by spin order transfer to 1-¹³C and ester hydrolysis, hyperpolarized 1-¹³C-Pyr should be formed.

Vinylesters are synthesized on an industrial scale as monomers for the production of polymers. The most important process is the reaction of ethylene with acetic acid in the presence of air and a Pd metal catalyst.^[36] Vinyl esters of higher carboxylic acids or substituted carboxylic acids are more difficult to prepare and usually are synthesized by transvinylation of the corresponding carboxylic acid with vinyl acetate and a transition metal catalyst.^[37] Hg(II) salts,^[38] Pd(II) salts,^[39] Pd(II) complexes,^[40–43] Au(I) complexes^[44] and Ru(III) complexes^[45] have been used towards this end. However, high temperatures and a large excess of the vinylation reagent are necessary to achieve reasonable yields, and the separation from unreacted vinylation reagents, polymerization or other byproducts are major problems in most procedures. Even more problematic is the synthesis of vinylesters of α- and β-ketocarboxylic acids, which are base sensitive or susceptible to decarboxylation under acidic conditions.

Two procedures have been published describing the synthesis of pyruvic acid vinylester. Both procedures start from pyruvic acid. The first reaction uses the known palladium catalyzed trans vinylation procedure with a large excess of vinyl acetate (**Figure 1a**). However, unlike aliphatic carboxylic acids, the α-ketocarboxylic acid, pyruvic acid gives only 6% yield.^[30] The strongly basic reaction conditions favor dimerization and oligomerization of the product via Aldol reactions, reducing the yield and giving rise to a reaction mixture, which is difficult to purify. Consequently, the second published synthesis tries to avoid these side reactions by transforming the keto group (position 1 in pyruvic acid) into the diethyl acetal, and by applying an optimized transvinylation procedure.^[46] While improving the transvinylation process, the two additional steps, the acetalization of pyruvic acid in the first step, and the hydrolysis of the acetal after transvinylation, reduce the overall yield to 8.2%. The product was contaminated with ethyl pyruvate but was used for successful hyperpolarization experiments.^[45]

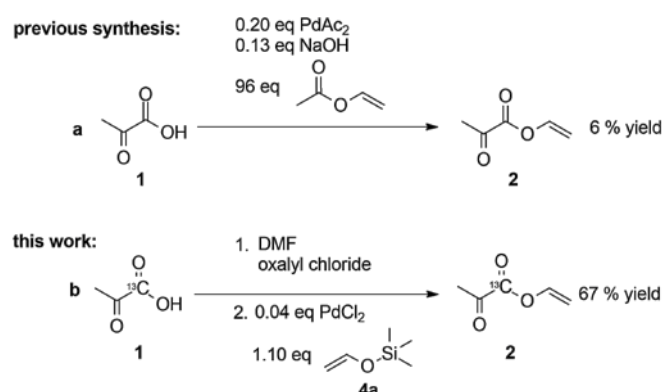


Figure 1. Synthesis of vinyl pyruvate. (a) Preparation by Chukanov et al.^[30], where the vinyl group is transferred from vinylacetate to pyruvate (transvinylation) in the presence of palladium(II). (b) Our new synthesis uses a vinyloxy silane (**4**) as a vinyl source. Significantly improved yields of vinyl pyruvate were achieved. The method was easily modified to obtain also isotopically labeled molecules. DMF = dimethylformamide.

Except vinyl pyruvate only one α-ketocarboxylic acid vinylester is known,^[47] and the synthetic procedure is not suitable for large-scale preparations, or for the synthesis of labelled compounds. Vinyl esters of 1,3-ketocarboxylic acids cannot be synthesized by the usual vinylation or transvinylation methods at all (see above). Only vinyl acetoacetate has been synthesized, however, by high temperature pyrolysis in moderate yields.^[48,49]

Here, we present a new strategy for the synthesis of ketocarboxylic acid vinyl esters (**Figure 1b**), and prepared different ¹³C and ²H (D) labeled vinyl pyruvates (**Figure 2**). We achieved 67% yield for 1-¹³C-vinyl pyruvate and 17% for 1-¹³C-vinyl pyruvate-*d*6. Other isotopomers were synthesized as well. We successfully conducted PHIP of these agents, and accomplished a ¹³C-polarization of 12% for 1-¹³C-ethyl pyruvate-*d*6 after hydrogenation with 50% pH₂. With 100 % enriched pH₂ the polarization yield is expected to triple to more than 30%.

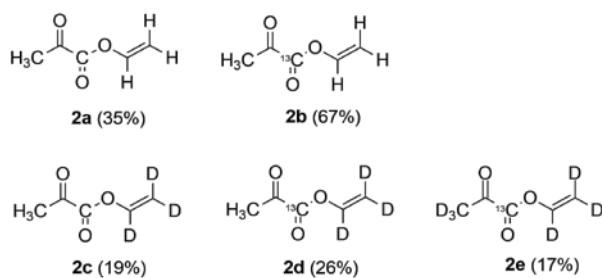


Figure 2. Synthesized isotopomers of vinyl pyruvate and the corresponding yields: vinyl pyruvate (**2a**), $1\text{-}^{13}\text{C}$ -vinyl pyruvate (**2b**), vinyl pyruvate- d_3 (**2c**), $1\text{-}^{13}\text{C}$ -vinyl pyruvate- d_3 (**2d**), $1\text{-}^{13}\text{C}$ -vinyl pyruvate- d_6 (**2e**).

Results and Discussion

Synthesis

The preparation starts by transforming the pyruvic acid into the corresponding acid chloride (**3a-c**) using the Vilsmeier-Haack reagent^[50] with oxalyl chloride and catalytic amounts of *N,N*-dimethylformamide. Alternative procedures described in the literature provided lower yields and side products that were difficult to remove.^[51–54] The acid chloride was then used as a raw product in the next reaction step. As vinyllating agents, vinyloxy silanes (**4a-c**) were used in the presence of a palladium catalyst. The resulting vinyl esters (**2a-e**) could be isolated by flash column purification. Vinyloxy-trimethylsilane is very moisture sensitive but more reactive than more hindered derivatives. Vinyloxy-dimethyl-isopropylsilane turned out to be a good compromise between stability and reactivity.

Several transition metal catalysts were tested. Only HgCl_2 and especially PdCl_2 gave satisfying yields, with PdCl_2 being superior to $\text{Pd}(\text{OAc})_2$. Dichloromethane (DCM) was the solvent of choice.

According to this scheme, vinyl pyruvate- H_6 (**2a**) and $1\text{-}^{13}\text{C}$ -vinyl pyruvate- H_6 (**2b**) were prepared for the first time in high yields and high purity in just two consecutive steps (**Figure 3**). All reactions were carried out starting with 1 g of (^{13}C labelled and unlabeled) pyruvic acid. The isolated yield of vinyl pyruvate (**2b**) was 65%. The raw yield was determined by NMR to be up to 90%. Vinyl pyruvates are very sensitive to acidic and particularly basic conditions. The isolated yields therefore depended decisively on the workup procedure (see Supporting Information). Because of the very mild reaction conditions, the yields compared to established procedures were improved by a factor of eight.^[30] Even if a significant amount of vinyl pyruvate (**2**) was lost during the workup procedure, the isolated vinyl pyruvate (**2**) exhibited a higher purity than reported.^[46] The procedure is especially suitable for small batches in the range of hundreds of milligrams to several grams, making it ideal for producing small amounts of isotopically labeled substances starting from the corresponding acids.

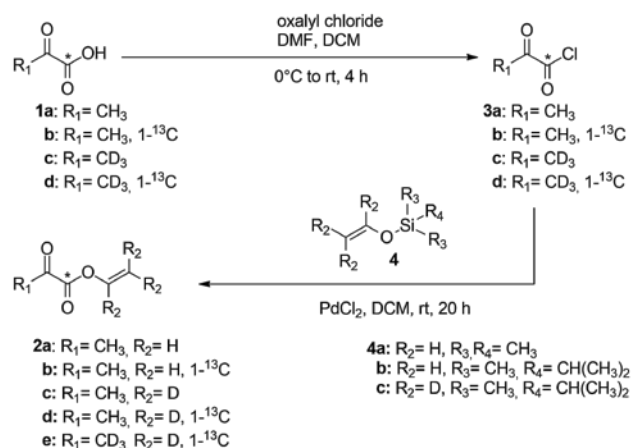


Figure 3. General reaction scheme for the synthesis of vinyl pyruvates. First, the carboxylic acid (**1a-c**) was converted to the acid chloride (**3a-c**). Then catalytic amounts of PdCl_2 were added and vinyloxy silane (**4a-c**) was used as a vinyllating agent to produce vinyl pyruvate (**2a-e**). The C-1 position is marked with a star. DCM = dichloromethane, DMF = dimethylformamide.

For hyperpolarization experiments, the ^{13}C -labelled and fully deuterated $1\text{-}^{13}\text{C}$ -vinyl-pyruvate- d_6 (**2e**, $1\text{-}^{13}\text{C}$ -VP- d_6 , **Figure 4**) is the most promising precursor (see above). $1\text{-}^{13}\text{C}$ -pyruvate- d_4 (**1c**, **Figure 3**) and dimethylisopropyl(vinyloxy) silane- d_3 (**4c**) were used as starting compounds to synthesize $1\text{-}^{13}\text{C}$ -VP- d_6 . Based on a procedure reported by Denmark et al.,^[55] we developed a synthetic route to obtain deuterated vinyloxysilane **4c** using tetrahydrofuran- d_8 (THF- d_8 , **5**) as a deuterium source. THF- d_8 (**5**) was cleaved with *n*-butyllithium (*n*-BuLi) and the generated enolate (**6**) of acetaldehyde was trapped with a trialkylsilyl chloride to obtain the deuterated trialkyl(vinyloxy)silane (**Figure 4**). It is noteworthy that a considerable kinetic isotope effect was observed in the cleavage of THF- d_8 and the reaction times with BuLi had to be extended. The silane (**4c**) was subsequently reacted with the pyruvyl chloride to the target product **1c**. Since trimethyl(vinyloxy)silane (**4a**) is very sensitive to water, and because its boiling point (75°C) is close to the one of THF (67°C), separation was not possible on a small scale. We therefore used dimethylisopropyl(vinyloxy)silane (**4b-c**) (b.p. 137°C), which was obtained in high yields and purity as d_3 -derivate (**4c**) after a simple workup procedure.

From 1 g (10.9 mmol) of $1\text{-}^{13}\text{C}$ -Pyr- d_4 (**1c**), we obtained 222 mg (1.85 mmol) of $1\text{-}^{13}\text{C}$ -VP- d_6 (**2e**) which was further investigated in PHIP-SAH experiments. The total yield over two steps was determined to be 17% relative to $1\text{-}^{13}\text{C}$ -Pyr- d_4 .

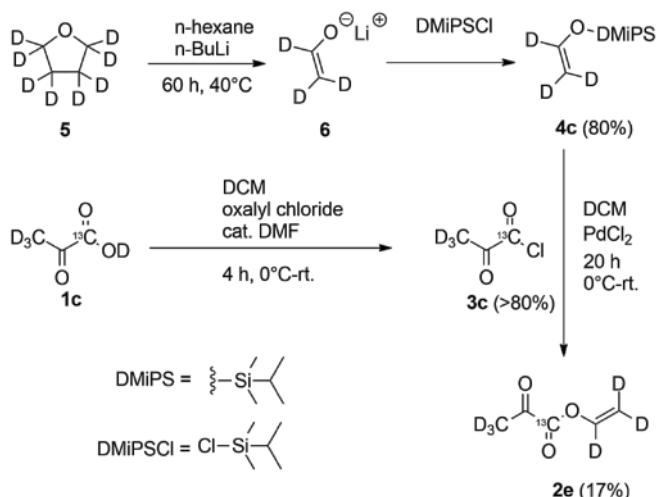


Figure 4. Synthesis of 1-¹³C-vinyl pyruvate-*d*₆. 1-¹³C-VP-*d*₆ 2e was prepared using dimethyl isopropyl (vinyloxy)silane as vinyl source. Purification was performed after the last reaction step.

Hyperpolarization

Parahydrogenation and subsequent spin order transfer and cleavage of side arms (**Figure 5**) were carried out at a probe temperature of 330 K, in chloroform-*d*, at a magnetic field of 9.4 T, with 50 % p_{H₂}^[56] and a hydrogenation time of $t_{h_2} = 20$ s (see experimental section for more details).

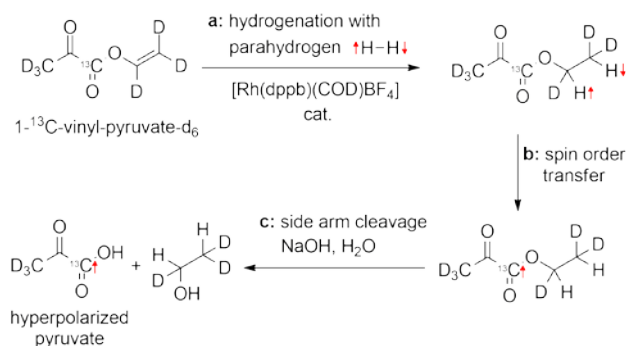


Figure 5. Pyruvate PHIP-SAH hyperpolarization. (a) Parahydrogen was added to 1-¹³C-VP-*d*₆ in chloroform-*d* and in the presence of homogeneous catalyst [Rh(dppb)(COD)BF₄] (dppb = 1,4-Bis(diphenylphosphino)butane). (b) Then using spin order transfer method p_{H₂} spin order is converted to net magnetization of 1-¹³C nucleus of pyruvate. (c) And finally, aqueous NaOH solution is added to cleave the side arm. As a result hyperpolarized 1-¹³C-Pyr in aqueous phase is produced.

Upon hydrogenation of 1-¹³C-VP-*d*₆, 1-¹³C-ethyl pyruvate-*d*₆ (1-¹³C-EP-*d*₆) was produced (**Figure 6a**). As expected, the ¹H spectrum exhibited two pairs of hyperpolarized, antiphase lines corresponding to methylene (CDH) and methyl (CD₂H) sites 1-¹³C-EP-*d*₆ after a hard 45° excitation (**Figure 6b1**, PASADENA experiment). The average enhancement of each line was $\epsilon l = 2100$, corresponding to a multiplet polarization $mP = 12.2\%$. The multiplet polarization mP of two spins corresponds to $\frac{1}{4} - mP \cdot \hat{I}_Z^1 \hat{I}_Z^2$ density matrix and therefore also referred to as ZZ-spin

order). The maximum multiplet polarization of two protons that can be achieved theoretically by the addition of 50% p_{H₂} is $P^{1H} = 33.3\%$ ^[57] only ~ 2.7 times higher than what was achieved experimentally. The main polarization losses are usually considered singlet-triplet mixing on the catalyst and relaxation^[58,59].

Using a series of small flipping angles $\varphi = 5^\circ$ with a repetition time TR = 4 s, we quantified the lifetime of the multiplet polarization to $T_{HP}^{ZZ} = 30.9$ s (observed value 30.5 s, **Figure 6b2**). Using this constant to estimate the polarization at the beginning of the hydrogenation period (eq. 1) yielded an initial polarization of 18.8 % - accounting for some, but not the complete difference to the theoretical maximum of 33.3%.

$$P = \exp[-t_{h_2}/T_{HP}^{ZZ}] \cdot P_{max} \quad (\text{eq. 1})$$

Using “efficient spin order transfer to heteronuclei via a relayed INEPT chains” (ESOTHERIC)^[21] allowed us to achieve ~ 12% ¹³C-polarization of 1-¹³C-EP-*d*₆, a 16500 fold enhancement with respect to the thermal equilibrium at 9.4 T. By using 100% p_H instead of 50%, these numbers are expected to triple.

The lifetime of the polarization in chloroform-*d* at 9.4 T was measured to ~ 27.2 s (26.5 s observed value, **Figure 6c**), less than expected e.g. in water, and maybe caused by the detrimental effect of Cl containing solvents as recently reported^[60]. Here, it was essential to clean the high-pressure tube with concentrated nitric acid before the experiment; - otherwise, T₁ was found to decrease further (down to ~ 15 s). This effect may be attributed to a grey film which appeared on the surface of the tube if chloroform was used for flushing instead, and which did not dissolve in organic solvents like acetone, chloroform, or ethanol.

For any in vivo application of hyperpolarized contrast agents, it is necessary to extract the hyperpolarized contrast agent from the solution of the organic solvent and the metal-organic catalyst. Here, we used the established two-phase approach described before.^[31] After hydrogenation and SOT at 9.4 T, the sample was flushed into another NMR tube outside of the magnet, containing water (83% D₂O and 17% H₂O) and 167 mM NaOH. This tube was shaken and inserted into the NMR spectrometer again. We did this outside to mimic an envisaged experiment where hyperpolarized media will be manipulated manually and administrated outside of the magnet.

A single, strong ¹³C resonance was observed at 170.3 ppm, the expected frequency of pyruvate. No signal was observed at 161 ppm, the expected resonance of 1-¹³C-EP.^[27,31] More interestingly, the lifetime of the hyperpolarized pyruvate signal was found to increase to 72.7 s (68 s observed, **Figure 6e**) – expected for pyruvate in aqueous solution, and sufficiently long to reduce relaxation during administration.

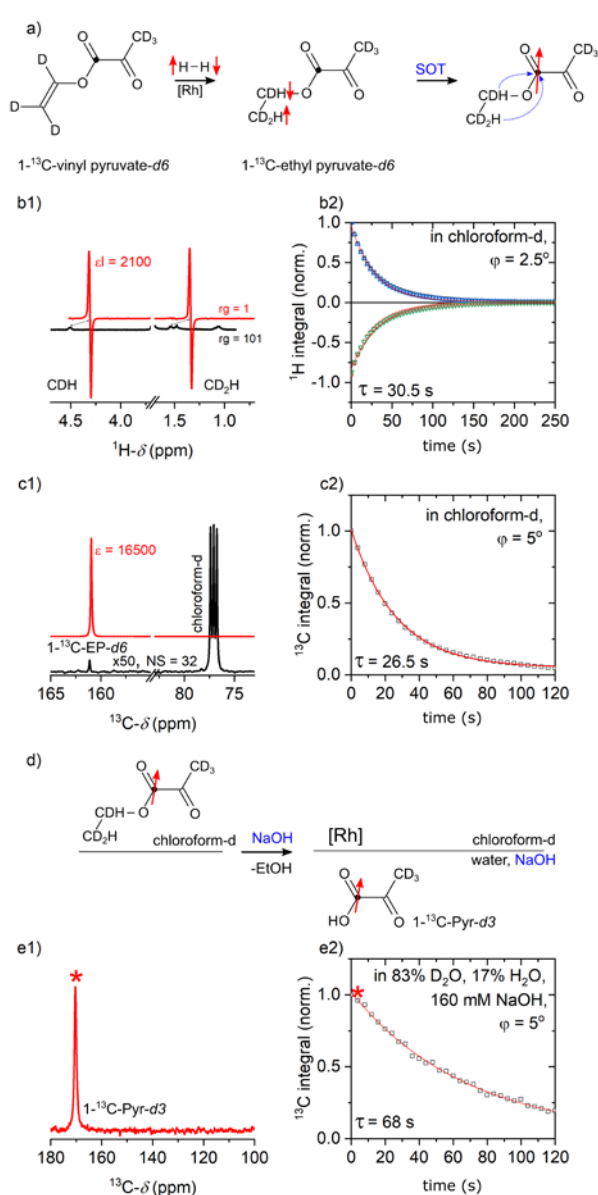


Figure 6 Hyperpolarization of $1\text{-}^{13}\text{C}$ -ethyl pyruvate- d_6 and $1\text{-}^{13}\text{C}$ -pyruvate- d_3 . (a) Schematic view of the addition of $p\text{H}_2$ (red arrows) to $1\text{-}^{13}\text{C}$ -VP- d_6 yielding $1\text{-}^{13}\text{C}$ -EP- d_6 and subsequent spin order transfer (SOT) using the J-coupling network to obtain ^{13}C polarization (red arrow). (b) Hyperpolarized ^1H -PASADENA (red) and corresponding thermal spectrum (black) acquired with receiver gains (rg) 1 and 101. The average line enhancement was $\epsilon l = 2100$ at 9.4 T (the black thermal signal was moved 0.2 ppm to the left for better visualization). The decaying magnetization was sampled with a train of small flip angle pulses and a monoexponential function was fitted to the data, yielding an observable ZZ-spin order decay $\tau = 30.5$ s. (c) After the SOT to ^{13}C , a signal enhancement of 16500 or 12% polarization of $1\text{-}^{13}\text{C}$ -EP- d_6 was obtained (Figure 6, parameters $\tau_1 = \tau_3 = 84$ ms and $\tau_2 = 36$ ms). The observable signal decay was $\tau = 26$ s. The thermal spectrum was enlarged 50 fold and measured with the same acquisition parameters using 32 scans and a repetition time of 200 s. (d) Scheme of two-phase separation and sidearm cleavage as a result of the addition of NaOH aqueous solution. (e1) ^{13}C -NMR spectrum of aqueous phase showing strong ^{13}C -signal of hyperpolarized pyruvate after cleavage, the first in a row used to sample the decaying polarization (e2). The observable lifetime of $1\text{-}^{13}\text{C}$ -Pyr- d_3 was extended to $\tau =$

68 s in aqueous solution. Note that all three hyperpolarization decays (b2, c2, e2) were measured with repetition time $\text{TR} = 4$ s and an excitation angle of 5° (2.5° used for PASADENA is equivalent to 5° used for magnetization). Corresponding corrected hyperpolarization lifetime values do not significantly differ from observed values: 30.9 s, 27.2 s and 72.7 s.

Conclusion

We present a significantly improved synthesis of vinyl esters of α -ketocarboxylic acids, particularly of vinyl pyruvate. In contrast to previous methods, which depend on a very large excess of vinylacetate and addition of a base, we use equimolar amounts of vinyloxysilylanes as the vinyl source for transvinylation. The reaction proceeds at room temperature under PdCl_2 catalysis and under neutral or slightly acidic conditions, which prevents dimerization and oligomerization of the base-sensitive vinyl esters. The high yields and simple workup are particularly suitable for the preparation of isotopically labelled vinyl pyruvates. Five different deuterium and ^{13}C labelled vinyl pyruvates were prepared, including the fully deuterated and $1\text{-}^{13}\text{C}$ labelled vinyl pyruvate. The latter compound is ideally suited for the preparation of hyperpolarized pyruvate via PHIP-SAH method. Hyperpolarization yields as high as 12% were obtained with 50% parahydrogen, which corresponds to a gain of factor 16 500 in intensity of the $1\text{-}^{13}\text{C}$ signal at 9.4 T magnet. With 100% parahydrogen a polarization of 36% is expected. Polarization rates in this range, to date, were only obtained by the much more expensive and elaborate DNP method. DNP-hyperpolarized pyruvate has been used to monitor the metabolism of pyruvate to lactate by MRI in vivo. The conversion of pyruvate to lactate and other metabolites is faster in prostate and breast cancer cells (Warburg effect). This molecular imaging method has high prospects for the early detection of cancer before structural or anatomical changes are visible in conventional MRI. Our synthetic method now provides access to the suitable precursor for the convenient and cost-effective PHIP method, which allows hyperpolarization of pyruvate at much reduced cost, with less sophisticated instrumentation and significantly higher throughput and thus brings hyperpolarization closer to clinical applications.

ASSOCIATED CONTENT

Detailed synthetic procedures and analytical data of all substances are available in the supporting information

AUTHOR INFORMATION

Corresponding Author

A. Brahms: abrahms@oc.uni-kiel.de, R.Herges: rherges@oc.uni-kiel.de

Dr. A. N. Pravdivtsev: andrey.pravdivtsev@rad.uni-kiel.de

Author Contributions

AB, ANP, JBH, RH: conceptualization, writing – original draft. AB, RH conceptualization of VP synthesis. AB, RH and TS investigation of VP synthesis. FS analysis of NMR during VP synthesis. ANP, FE investigation of EP hyperpolarization. ANP, RH, FS and JBH: supervision, funding acquisition. All authors contributed to discussions and helped interpreting the results and have given

approval to the final version of the manuscript. ‡These authors contributed equally

Funding Sources

We acknowledge funding from German Federal Ministry of Education and Research (BMBF) within the framework of the e:Med research and funding concept (01ZX1915C), DFG (PR 1868/3-1, HO-4602/2-2, HO-4602/3, GRK2154-2019, EXC2167, FOR5042, SFB1479, TRR287). MOIN CC was founded by a grant from the European Regional Development Fund (ERDF) and the Zukunftsprogramm Wirtschaft of Schleswig-Holstein (Project no. 122-09-053).

Notes

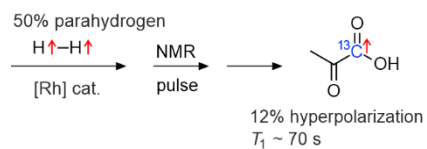
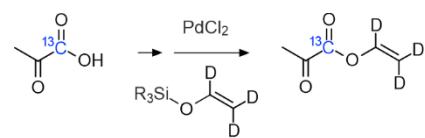
ACKNOWLEDGMENT

We acknowledge funding from German Federal Ministry of Education and Research (BMBF) within the framework of the e:Med research and funding concept (01ZX1915C), DFG (PR 1868/3-1, HO-4602/2-2, HO-4602/3, GRK2154-2019, EXC2167, FOR5042, SFB1479, TRR287). MOIN CC was founded by a grant from the European Regional Development Fund (ERDF) and the Zukunftsprogramm Wirtschaft of Schleswig-Holstein (Project no. 122-09-053)

REFERENCES

- [1] C. Thomsen, U. Becker, K. Winkler, P. Christoffersen, M. Jensen, O. Henriksen, *Magn. Reson. Imaging* **1994**, *12*, 487–495.
- [2] W. Heil, C. Gemmel, S. Karpuk, Y. Sobolev, K. Tullney, F. Allmendinger, U. Schmidt, M. Burghoff, W. Kilian, S. Knappe-Grüneberg, A. Schnabel, F. Seifert, L. Trahms, *Ann. Phys.* **2013**, *525*, 539–549.
- [3] A. Dey, B. Charrier, E. Martineau, C. Deborde, E. Gandriaux, A. Moing, D. Jacob, D. Eshchenko, M. Schnell, R. Melzi, D. Kurzbach, M. Ceillier, Q. Chappuis, S. F. Cousin, J. G. Kempf, S. Jannin, J.-N. Dumez, P. Giraudeau, *Anal. Chem.* **2020**, *92*, 14867–14871.
- [4] H. Kovacs, D. Moskau, M. Spraul, *Prog. Nucl. Magn. Reson. Spectrosc.* **2005**, *46*, 131–155.
- [5] E. Luchinat, L. Barbieri, M. Cremonini, L. Banci, *J. Biomol. NMR* **2021**, *75*, 97–107.
- [6] A. Abragam, J. M. Winter, *Phys. Rev. Lett.* **1958**, *1*, 374–375.
- [7] J. H. Ardenkjær-Larsen, B. Fridlund, A. Gram, G. Hansson, L. Hansson, M. H. Lerche, R. Servin, M. Thaning, K. Golman, *PNAS* **2003**, *100*, 10158–10163.
- [8] A. S. Lilly Thankamony, J. J. Wittmann, M. Kaushik, B. Corzilius, *Prog. Nucl. Magn. Reson. Spectrosc.* **2017**, *102–103*, 120–195.
- [9] S. J. Nelson, J. Kurhanewicz, D. B. Vigneron, P. E. Z. Larson, A. L. Harzstark, M. Ferrone, M. van Criekinge, J. W. Chang, R. Bok, I. Park, G. Reed, L. Carvajal, E. J. Small, P. Munster, V. K. Weinberg, J. H. Ardenkjær-Larsen, A. P. Chen, R. E. Hurd, L.-I. Odegaardstuen, F. J. Robb, J. Tropp, J. A. Murray, *Sci. Transl. Med.* **2013**, *5*, 198ra108–198ra108.
- [10] F. A. Gallagher, R. Woitek, M. A. McLean, A. B. Gill, R. M. Garcia, E. Provenzano, F. Riemer, J. Kaggie, A. Chhabra, S. Ursprung, J. T. Grist, C. J. Daniels, F. Zaccagna, M.-C. Laurent, M. Locke, S. Hilborne, A. Frary, T. Torheim, C. Bournsnel, A. Schiller, I. Patterson, R. Slough, B. Carmo, J. Kane, H. Biggs, E. Harrison, S. S. Deen, A. Patterson, T. Lanz, Z. Kingsbury, M. Ross, B. Basu, R. Baird, D. J. Lomas, E. Sala, J. Wason, O. M. Rueda, S.-F. Chin, I. B. Wilkinson, M. J. Graves, J. E. Abraham, F. J. Gilbert, C. Caldas, K. M. Brindle, *PNAS* **2020**, *117*, 2092–2098.
- [11] M. V. Liberti, J. W. Locasale, *Trends Biochem. Sci.* **2016**, *41*, 211–218.
- [12] H. Gutte, A. E. Hansen, H. H. Johannesen, A. E. Clemmensen, J. H. Ardenkjær-Larsen, C. H. Nielsen, A. Kjær, *Am. J. Nuc. Med. Mol. Imag.* **2015**, *5*, 548–560.
- [13] C. R. Bowers, D. P. Weitekamp, *J. Am. Chem. Soc.* **1987**, *109*, 5541–5542.
- [14] J.-B. Hövener, A. N. Pravdivtsev, B. Kidd, C. R. Bowers, S. Glöggler, K. V. Kovtunov, M. Plaumann, R. Katz-Brull, K. Buckenmaier, A. Jerschow, F. Reineri, T. Theis, R. V. Shchepin, S. Wagner, P. Bhattacharya, N. M. Zacharias, E. Y. Chekmenev, *Angew. Chem. Int. Ed.* **2018**, *57*, 11140–11162.
- [15] B. Feng, A. M. Coffey, R. D. Colon, E. Y. Chekmenev, K. W. Waddell, *J. Magn. Reson.* **2012**, *214*, 258–262.
- [16] A. V. Zhuzhgov, O. P. Krivoruchko, L. A. Isupova, O. N. Mart'yanov, V. N. Parmon, *Catal. Ind.* **2018**, *10*, 9–19.
- [17] A. B. Schmidt, J. Wörner, A. Pravdivtsev, S. Knecht, H. Scherer, S. Weber, J. Hennig, D. von Elverfeldt, J.-B. Hövener, *ChemPhysChem* **2019**, *20*, 2408–2412.
- [18] M. Goldman, H. Jóhannesson, *C. R. Phys.* **2005**, *6*, 575–581.
- [19] A. N. Pravdivtsev, A. V. Yurkovskaya, N. N. Lukzen, K. L. Ivanov, H.-M. Vieth, *J. Phys. Chem. Lett.* **2014**, *5*, 3421–3426.
- [20] A. B. Schmidt, S. Berner, W. Schimpf, C. Müller, T. Lickert, N. Schwaderlapp, S. Knecht, J. G. Skinner, A. Dost, P. Rovedo, J. Hennig, D. von Elverfeldt, J.-B. Hövener, *Nat. Commun.* **2017**, *8*, ncomms14535.
- [21] S. Korchak, S. Mamone, S. Glöggler, *ChemistryOpen* **2018**, *7*, 672–676.
- [22] T. Theis, M. Truong, A. M. Coffey, E. Y. Chekmenev, W. S. Warren, *J. Magn. Reson.* **2014**, *248*, 23–26.
- [23] A. N. Pravdivtsev, A. V. Yurkovskaya, H. Zimmermann, H.-M. Vieth, K. L. Ivanov, *Chem. Phys. Lett.* **2016**, *661*, 77–82.
- [24] J. F. P. Colell, A. W. J. Logan, Z. Zhou, R. V. Shchepin, D. A. Barskiy, G. X. Ortiz, Q. Wang, S. J. Malcolmson, E. Y. Chekmenev, W. S. Warren, T. Theis, *J. Phys. Chem. C* **2017**, *121*, 6626–6634.
- [25] R. W. Adams, J. A. Aguilar, K. D. Atkinson, M. J. Cowley, P. I. P. Elliott, S. B. Duckett, G. G. R. Green, I. G. Khazal, J. López-Serrano, D. C. Williamson, *Science* **2009**, *323*, 1708–1711.
- [26] I. V. Koptug, K. V. Kovtunov, S. R. Burt, M. S. Anwar, C. Hilty, S.-I. Han, A. Pines, R. Z. Sagdeev, *J. Am. Chem. Soc.* **2007**, *129*, 5580–5586.
- [27] F. Reineri, T. Boi, S. Aime, *Nat. Commun.* **2015**, *6*, ncomms6858.
- [28] L. Kaltschnee, A. P. Jagtap, J. McCormick, S. Wagner, L.-S. Bouchard, M. Utz, C. Griesinger, S. Glöggler, *Chem. Eur. J.* **2019**, *25*, 11031–11035.
- [29] A. N. Pravdivtsev, G. Buntkowsky, S. B. Duckett, I. V. Koptug, J.-B. Hövener, *Angew. Chem. Int. Ed.* **2021**, *60*, 23496–23507.
- [30] N. V. Chukanov, O. G. Salnikov, R. V. Shchepin, K. V. Kovtunov, I. V. Koptug, E. Y. Chekmenev, *ACS Omega* **2018**, *3*, 6673–6682.
- [31] E. Cavallari, C. Carrera, M. Sorge, G. Bonne, A. Muchir, S. Aime, F. Reineri, *Sci. Rep.* **2018**, *8*, 8366.
- [32] E. Cavallari, C. Carrera, S. Aime, F. Reineri, *J. Magn. Reson.* **2018**, *289*, 12–17.
- [33] P. TomHon, M. Abdulmojeed, I. Adelabu, S. Nantogma, S. H. Kabir, S. Lehmkuhl, E. Y. Chekmenev, T. Theis, [10.33774/chemrxiv-2021-cpz32](https://doi.org/10.33774/chemrxiv-2021-cpz32) **n.d.**, 6.
- [34] E. Cavallari, C. Carrera, S. Aime, F. Reineri, *ChemPhysChem* **2019**, *20*, 318–325.
- [35] A. Pravdivtsev, J.-B. Hövener, A. B. Schmidt, *ChemPhysChem* **n.d.**, *n/a*, DOI 10.1002/cphc.202100721.
- [36] Y.-F. Han, D. Kumar, C. Sivadinarayana, D. W. Goodman, *J. Cat.* **2004**, *224*, 60–68.

- [37] F. J. Waller, in *Catalysis of Organic Reactions, Chapter 26*, J. R. Kosak, T. A. Johnson, Eds., CRC Press, **1994**.
- [38] R. L. Adelman, *J. Org. Chem.* **1949**, *14*, 1057–1077.
- [39] J. Smidt, A. Sabel, *Production of Vinyl Esters*, **1965**, US3188319A.
- [40] J. E. McKeon, P. Fitton, *Tetrahedron* **1972**, *28*, 233–238.
- [41] A. A. Ketterling, A. S. Lisitsyn, A. V. Nosov, V. A. Likholobov, *Appl. Cat.* **1990**, *66*, 123–131.
- [42] L. Johnen, H. Strutz, *Transvinylierung Als Erste Stufe Einer Koppelproduktion von Vinylestern Und Essigsäure- Oder Propionsäurefolgeprodukten*, **2013**, WO2013117295A1.
- [43] I. M. Nunez, D. E. Seelye, *Process for Preparing Vinyl Chloroformate*, **2013**, WO2013003318A1.
- [44] A. Nakamura, M. Tokunaga, *Tetrahedron Lett.* **2008**, *49*, 3729–3732.
- [45] J. Ziriakus, T. K. Zimmermann, A. Pöthig, M. Drees, S. Haslinger, D. Jantke, F. E. Kühn, *Adv. Synth. Catal.* **2013**, *355*, 2845–2859.
- [46] C. Carrera, E. Cavallari, G. Digilio, O. Bondar, S. Aime, F. Reineri, *ChemPhysChem* **2021**, *22*, 1042–1048.
- [47] S. Hu, D. C. Neckers, *J. Org. Chem.* **1997**, *62*, 7827–7831.
- [48] J. A. Hyatt, *J. Org. Chem.* **1984**, *49*, 5102–5105.
- [49] H. D. Eck, H. D. Spes, *Vinylacetoacetates - Prepd by Pyrolysis of Acetoacetates*, **1973**, DE2142419A1.
- [50] G. Jones, S. P. Stanforth, in *Organic Reactions*, John Wiley & Sons, Ltd, **2004**, pp. 355–686.
- [51] A. Devos, J. Remion, A.-M. Frisque-Hesbain, A. Colens, L. Ghosez, *J. Chem. Soc., Chem. Commun.* **1979**, 1180–1181.
- [52] H. C. J. Ottenheijm, M. W. Tjihuis, *Org. Synth.* **1983**, *61*, 1.
- [53] J. Häusler, U. Schmidt, *Chem. Ber.* **1974**, *107*, 2804–2815.
- [54] P. Biju, *Synth. Commun.* **2008**, *38*, 1940–1945.
- [55] S. E. Denmark, T. Bui, *J. Org. Chem.* **2005**, *70*, 10190–10193.
- [56] F. Ellermann, A. Pravdivtsev, J.-B. Hövener, *Magn. Reson.* **2021**, *2*, 49–62.
- [57] A. N. Pravdivtsev, F. Ellermann, J.-B. Hövener, *Phys. Chem. Chem. Phys.* **2021**, *23*, 14146–14150.
- [58] J. Natterer, J. Bargon, *Prog. Nucl. Magn. Reson. Spectrosc.* **1997**, *31*, 293–315.
- [59] S. Berner, A. B. Schmidt, M. Zimmermann, A. N. Pravdivtsev, S. Glöggler, J. Hennig, D. von Elverfeldt, J.-B. Hövener, *ChemistryOpen* **2019**, *8*, 728–736.
- [60] A. Jerschow, B. Kharkov, X. Duan, J. Rantaharju, M. Sabba, M. Levitt, J. Canary, **2021**, DOI 10.26434/chemrxiv-2021-7bgpc.
- [61] A. B. Schmidt, A. Brahms, F. Ellermann, S. Knecht, S. Berner, J. Hennig, D. von Elverfeldt, R. Herges, J.-B. Hövener, A. Pravdivtsev, *Phys. Chem. Chem. Phys.* **2021**, DOI 10.1039/D1CP04153C.



Hyperpolarized pyruvate is a highly promising tracer for in vivo metabolic MRI. A new synthetic approach provides access to the key precursor of ^{13}C labelled vinyl pyruvate with up to 67% yield (8 times higher than previous methods). After spin order transfer with parahydrogen, 12% ^{13}C polarization was obtained, which corresponds to a signal gain in NMR and MRI of 16 500 (9.4 T).

Institute and/or researcher Twitter usernames: @theMOINCC, @RainerHerges

Supporting information for

Synthesis and hyperpolarization of ^{13}C and ^2H labeled vinyl pyruvate and pyruvate

Arne Brahms^{[a]†*}, Andrey N. Pravdivtsev^{[b]†*}, Tim Stamp^[a], Frowin Ellermann^[b], Frank D. Sönnichsen^[a], Jan-Bernd Hövener^{[b] ‡}, Rainer Herges^{[a]‡*}

[a] A. Brahms, Prof. Dr. F. Sönnichsen, Prof. Dr. R. Herges
Otto Diels Institute for Organic Chemistry, Kiel University
Kiel University, Otto- Hahn Platz 4, 24098 Kiel, Germany
E-mail: abrahms@oc.uni-kiel.de, rherges@oc.uni-kiel.de

[b] Dr. A. N. Pravdivtsev, Prof. Dr. J.-B. Hövener, F. Ellermann
Section Biomedical Imaging, Molecular Imaging North Competence Center (MOIN CC)
IDepartment of Radiology and Neuroradiology, University Medical Center Kiel
Kiel University, Am Botanischen Garten 14, 24114, Kiel, Germany
E-mail: andrey.pravdivtsev@rad.uni-kiel.de, jan.hoeverner@rad.uni-kiel.de

†,‡ this authors contributed equally

* corresponding authors

Table of Content

1. Instrumentation	3
1.1 NMR	3
1.2 IR	3
1.3 List of chemicals	3
2. Synthesis details	4
2.1 Vinyloxy Silanes	4
2.1.1 Dimethylisopropyl(vinyloxy)silane (4b)	4
2.1.2 Dimethylisopropyl(vinyloxy)silane- <i>d</i> 3 (4c)	4
2.2 Vinyl pyruvates	5
2.2.1 Vinyl pyruvate with protonated sidearm (2a-b)	5
2.2.2 Vinyl pyruvate with deuterated sidearm (2c-e)	6
3. PHIP experimental details	7
3.1 PHIP sample processing	7
3.2 PHIP NMR experimental details	7
4. Spectroscopic data	9
4.1 Vinyloxy silanes	9
4.1.1 Vinyloxy silanes: dimethylisopropyl(vinyloxy)silane (4b)	9
4.1.2 Vinyloxy silanes: dimethylisopropyl(vinyloxy)silane- <i>d</i> 3 (4c)	10
4.2 Vinyl pyruvates	11
4.2.1 Spectra of vinyl pyruvate (2a)	11
4.2.1 Spectra of 1- ¹³ C-vinyl pyruvate (2b)	12
4.2.3 Spectra of vinyl pyruvate- <i>d</i> 3 (2c)	13
4.2.4 Spectra of 1- ¹³ C-pyruvate- <i>d</i> 3 (2d)	14
4.2.5 Spectra of 1- ¹³ C-vinyl pyruvate- <i>d</i> 6 (2e)	15

1. Instrumentation

1.1 NMR

To record the NMR spectra, the samples were dissolved in the specified deuterated solvents. Tetramethyl silane (TMS) signal (0 ppm ^1H and ^{13}C resonance) or the resonance frequency of the respective solvent (chloroform-d, 7.26 ppm ^1H resonance and 77.16 ppm ^{13}C resonance) was used for calibration of chemical shifts. The resonance frequencies are given in parts per million (ppm) and the coupling constants are specified in Hertz (Hz).

We used Bruker AC 200 MHz and Bruker DRX 500 MHz high-resolution NMR spectrometers with 5 mm TXI probes to control the synthesis and purity.

We used Bruker AVANCE NEO 400MHz WB with 5 mm BBFO probe for pH_2 experiments.

1.2 IR

The infrared spectra were recorded using a Fourier transform IR spectrometer 1600 Series Perkin Elmer using an A531-G ATR-Golden-Gate-Diamond unit. The signal intensities were referenced the evaluation as w (weak), m (medium) and s (strong).

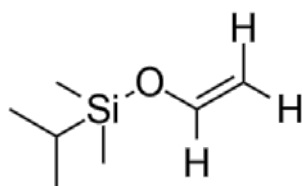
1.3 List of chemicals

Chemical	Manufacturer	Chemical purity (CP)
dichloromethane	Fisher Chemicals	99.8%
dimethylformamide (anhydrous)	Acros Organics	99.8%
dimethylisopropyl(vinyloxy)silane	TCI	>90%
tetrahydrofuran	Honeywell Riedel-de Haën	99.0%
tetrahydrofuran- <i>d</i> 8	Eurisotope	99.5%
trimethyl(vinyloxy)silane	TCI	>95.0%
oxalyl chloride	Alfa Aesar	98.0%
palladium(II)chloride	Sigma Aldrich	99.0%
pyruvic acid	TCI	95.0%
1- ^{13}C -pyruvic acid	Cambridge Isotope	≥ 99 atom % ^{13}C , $\geq 99\%$ (CP)
1- ^{13}C -pyruvic acid- <i>d</i> 4	Sigma Aldrich	≥ 99 atom % ^{13}C , ≥ 97 atom % D, $\geq 97\%$ (CP)

2. Synthesis details

2.1 Vinyloxy Silanes

2.1.1 Dimethylisopropyl(vinyloxy)silane (4b)

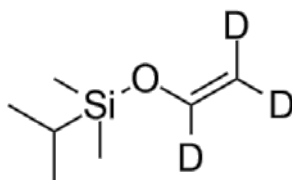


n-BuLi (7.33 ml, 80.65 mmol) was added dropwise to a cooled (0°C) solution of THF (26.1 ml, 323 mmol). After 0.5 h the solution was heated to 40°C and stirred for 20 h. The solution was again cooled to 0°C and dimethylisopropylsilyl chloride (13.0 ml, 82.7 mmol) was added slowly. After 2 h of stirring the solvent was removed i. vac. yielding a slurry containing lithium chloride. Diethyl ether was added and the organic phase was washed three times with half saturated sodium hydrogen carbonate solution and the resulting combined aqueous solution was extracted once with diethyl ether. The solvent was removed i. vac. and the product was obtained as a clear liquid with a yield of 6.59 g (57%).

¹H-NMR (500 MHz, CDCl₃, 298 K): δ = 6.51 (dd, ³J=13.61 Hz, ³J=5.85 Hz, 1 H, H-1), 4.43 (dd, ³J=13.61 Hz, ²J=0.76 Hz, 1 H, H-2), 4.11 (dd, ³J=5.85 Hz, ²J=0.76 Hz, 1H, H-2), 0.98 (m, 6 H, CH(CH₃)₂), 0.14 (s, 6 H, Si(CH₃)₂) ppm.

¹³C-NMR (500 MHz, CDCl₃, 298 K): δ = 146.17 (C-1), 94.42 (C-2), 16.57 (C-3,4), 14.43 (C-5), -4.41 (C-6,7).

2.1.2 Dimethylisopropyl(vinyloxy)silane-*d*3 (4c)



The product was obtained according to an analogous procedure as dimethylisopropyl(vinyloxy)silane. The only variation in the method was the use of 16.1 mL (198 mmol) THF-*d*8 instead of THF. After the addition of 4.51 mL (49.6 mmol) 11 M *n*-BuLi the solution was stirred for 3 days at 40°C (instead of 20 h with THF-*h*8). The subsequent processing was carried out analogously to the procedure described above. The product was obtained as a clear liquid with a yield of 5.21 g (73%).

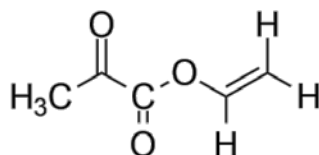
¹H-NMR (500 MHz, CDCl₃, 298 K): δ = 1.32 (m, 1 H, H-5), 0.98 (m, 6 H, CH(CH₃)₂), 0.15 (s, 6 H, SiC(CH₃)₂) ppm.

¹³C-NMR (500 MHz, CDCl₃, 298 K): δ = 16.75 (C-3,4), 14.60 (C-5), -4.23 (C-6,7) ppm.

2.2 Vinyl pyruvates

All syntheses were carried out according to the procedure optimized for undeuterated vinyl pyruvate. For the derivatives labelled with deuterium in the sidearm different equivalents and a different vinyloxy silane were used.

2.2.1 Vinyl pyruvate with protonated sidearm (2a-b)



To obtain the vinyl ester of pyruvic acid, DCM (10 ml) was placed in a three neck round bottom flask under N₂ atmosphere. The flask was cooled to 0°C and oxalyl chloride (0.974 ml, 11.4 mmol) was added. Afterwards pyruvic acid (0.787 ml, 11.4 mmol) and DMF (13 drops) were added as a solution in DCM (5 ml) in batches of 5 ml every 5 min. The solution was stirred for 2 h at 0°C and another 2 h at rt. The solution was degassed under Schlenk conditions and its volume reduced to 10 ml to obtain a solution of pyruvoyl chloride. Palladium(II)chloride (80.5 mg, 0.454 mmol) was placed in a round bottom flask under a N₂ atmosphere and brought into suspension with DCM (10 ml). The suspension was cooled to 0°C and commercially available trimethyl(vinyloxy)silane (**4a**) (1.87 ml, 12.5 mmol) was added. The mixture was stirred for 0.5 h and the freshly prepared solution of pyruvoyl chloride was added dropwise over 0.5 h. With no further cooling the solution was stirred for 20 h. Small amounts of hydroquinone were added and the solution was concentrated i. vac. to a volume of 3 mL, which was then purified via flash column chromatography on silica using DCM: *n*-pentane (20:80) (R_f= 0.6). The product was obtained with a yield of 871 mg (67 %) as a slightly yellow oil.

Vinyl pyruvate (2a):

yield: 443 mg (34%), purity: 93% (7 % EE)

¹H-NMR (500 MHz, CDCl₃, 298 K): δ = 7.28 (dd, ³J=13.84 Hz, ³J=6.17 Hz, 1H, *H*-4), 5.17 (dd, ³J=13.84 Hz, ²J=2.17 Hz, 1H, *H*-5), 4.83 (dd, ³J=6.17 Hz, ²J=2.17 Hz, 1H, *H*-5), 2.52 (s, 3H, CH₃) ppm.

¹³C-NMR (500 MHz, CDCl₃, 298 K): δ = 190.56 (C-2), 157.51 (C-2), 140.68 (C-5), 101.40 (C-4), 26.77 (C-3) ppm.

MS (ESI, MeOH): M/z (%) = 115.03 (42) [MH]⁺, 137.02 (100) [MNa]⁺, 169.05 (15) [M(MeOH)Na]⁺, 251.05 (44) [M2Na]⁺.

MS (HR): m/z (C₅H₆O₃Na⁺) = calc.: 137.02092, exp.: 137.02081 ± 110 ppm.

IR: λ (cm⁻¹) = 1829 (w), 1740 (s), 1648 (m), 1513 (w), 1362 (w), 1304 (w), 1139 (s), 1095 (w), 914 (w).

1-¹³C-vinyl pyruvate (2b)

yield: 859 mg (67%), purity: 76% (9 % DCM, 15 % EE)

¹H-NMR (500 MHz, CDCl₃, 298 K): δ = 7.27 (ddd, ³J=13.83 Hz, ³J=6.18 Hz, ³J=2.40 Hz, 1H, *H*-4), 5.12 (ddd, ³J=13.82, ²J=2.14 Hz, ⁴J=0.50 Hz, 1H, *H*-5), 4.82 (dd, ³J=6.17 Hz, ²J=2.17 Hz, 1H, *H*-5), 2.52 (d, ³J=1.57 Hz, 3H, CH₃) ppm.

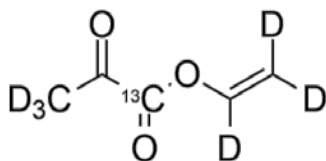
¹³C-NMR (500 MHz, CDCl₃, 298 K): δ = 190.53 (d, C-2), 157.50 (C-1), 140.66 (C-5), 101.39 (d, C-4), 26.80 (d, C-3) ppm.

MS (ESI, MeOH): M/z (%) = 138.02 (5) [Mna]⁺, 170.05 (11) [M(MeOH)Na]⁺.

MS (HR): m/z (C₄¹³CH₆O₃Na⁺) = calc.: 138.02427, exp.: 138.02421 ± 0.40 ppm.

IR: λ (cm⁻¹) = 3099 (w), 1719 (s), 1698 (s), 1645 (s), 1361 (w), 1298 (w), 1264 (w), 1235 (w), 1118 (s), 943 (w).

2.2.2 Vinyl pyruvate with deuterated sidearm (2c-e)



To obtain the 1-¹³C-vinyl pyruvate-*d*6, DCM (10 ml) was placed in a three necked round bottom flask under N₂ atmosphere. The flask was cooled to 0°C and oxalyl chloride (0.963 ml, 11.4 mmol) was added. Afterwards ¹³C-pyruvic acid (1 g, 11.2 mmol) and DMF (13 drops) were added as a solution in DCM (5 ml) in batches of 5 ml every 5 min. The solution was stirred for 2 h at 0°C and another 2 h at rt. The solution was degassed under Schlenk conditions and its volume reduced to 10 ml to obtain a solution of ¹³C-pyruvoyl chloride. Palladium(II)chloride (79.6 mg, 0.449 mmol) was placed in a round bottom flask under N₂ atmosphere and brought into suspension with DCM (10 ml). The suspension was cooled to 0°C and dimethylisopropyl(vinyloxy)silane-*d*3 (2.51 g, 17.0 mmol) was added. The mixture was stirred for 0.5 h and the prior prepared solution of pyruvoyl chloride was added dropwise over 0.5 h. With no further cooling the solution was stirred for 20 h. A pinch of hydroquinone was added and the solution was concentrated i. vac. to a volume of 3 mL, which were then purified via flash column chromatography on silica using DCM/*n*-pentane (20:80) (R_f=0.6). The product was obtained with a yield of 222 mg / 17%. The yield is lower than the yield of unlabeled vinyl pyruvate because more *n*-pentane was used during the gradient. We later found out that vinyl pyruvate forms an azeotrope with pentane and codestills upon removal of the solvents in a rotary evaporator, even though the boiling point difference of the two liquids is quite large (pentane: 36°C, vinyl pyruvate ~130°C). Codestillation can be prevented by adding the same volume of DCM.

Vinyl pyruvate-*d*3 (2c)

yield: 255 mg (19%), purity: 91% (4 % DCM, 5 % EE)

¹H-NMR (500 MHz, CDCl₃, 298 K): δ = 2.52 (s, 3 H, CH₃) ppm.

¹³C-NMR (500 MHz, CDCl₃, 298 K): δ = 190.54 (C-2), 157.48 (C-1), 26.75 (C-3).

MS (ESI, MeOH): M/z (%) = 118.06 (25) [M]⁺, 140.04 (44) [MNa]⁺.

MS (HR): m/z (C₅¹³CH₆O₃Na⁺) = calc.: 172.06596, meas.: 172.06576 ± 1.16 ppm.

IR: λ (cm⁻¹) = 2925 (w), 1736 (s), 1577 (w), 1421 (w), 1362 (s), 1293 (s), 1254 (s), 1131 (s), 1093 (s), 1018 (s), 687 (s), 600 (s).

1-¹³C-pyruvate-*d*3 (2d)

yield: 348 mg (26%), purity: 96% (1 % DCM, 3 % EE)

¹H-NMR (500 MHz, CDCl₃, 298 K): δ = 2.52 (d, ³J = 1.59 Hz, 3H, CH₃) ppm.

¹³C-NMR (500 MHz, CDCl₃, 298 K): δ = 190.40 (d, C-2), 157.48 (C-1), 140.43 (t, C-5), 100.73 (t, C-4), 26.60 (d, C-3) ppm.

MS (ESI, MeOH): M/z (%) = 141.04 (100) [MNa]⁺, 173.07 (14) [M(MeOH)Na]⁺.

MS (HR): m/z (C₅¹³CH₆O₃Na⁺) = calc.: 173.06932, meas.: 173.06917 ± 0.86 ppm.

IR: λ (cm⁻¹) = 2925 (w), 1740 (s), 1718 (s), 1697 (s), 1576 (s), 1421 (w), 1361 (m), 1271 (s), 1236 (s), 1018 (s), 980 (m), 953 (m), 687 (s), 623 (w), 600 (s)

1-¹³C vinyl pyruvate-*d*6 (2e)

yield: 222 mg (17%), purity: not evaluated.

²H-NMR (500 MHz, CDCl₃, 298 K): δ = 7.31 (s, 1D, D-4), 5.20 (s, 1D, D-5), 4.86 (s, 1D D-5), 2.50 (s, 3D, D-3) ppm.

¹³C-NMR (500 MHz, CDCl₃, 298 K): δ = 190.61 (d, C-2), 157.32 (s, C-1), 140.20 (t, C-5), 100.63 (t, C-4), 26.05 (d, C-3) ppm. IR: λ (cm⁻¹) = 3455 (w), 1735 (s), 1699 (s), 1575 (s), 1277 (m), 1137 (s), 1093 (s), 1006 (s), 959 (m), 689 (s), 645 (w), 543 (s)

3. PHIP experimental details

3.1 PHIP sample processing

PHIP-sample: The starting materials: 1-¹³C-vinyl pyruvate-*d6* (1-¹³C-VP-*d6*) and hydrogenation catalyst [1,4-Bis-(diphenylphosphino)-butan]-(1,5-cyclooctadiene)-rhodium(I)-tetrafluoroborate ([Rh], CAS 79255-71-3, Sigma Aldrich) were dissolved in 6 mL of chloroform-*d* (CAS 865-49-6, Sigma Aldrich). Resulting concentrations were 2 mM for 1-¹³C-VP-*d6* and [Rh]. 1-¹³C-VP-*d6* hydrogenates in the presence of 50% pH₂ [Rh] to 1-¹³C-ethyl pyruvate-*d6* (1-¹³C-EP-*d6*). 1-¹³C-VP-*d6* was used without additional purification after synthesis as described above.

PHIP experiment: All experiments were carried out in a 400 MHz wide-bore nuclear magnetic resonance (NMR) system (WB NMR 400 MHz, Avance Neo, 9.4 T, Bruker) using a 5 mm BBFO probe. Medium wall high-pressure 5 mm NMR tubes were used (524-PV-7, Wilmad-LabGlass). An inlet and outlet of the gas system were connected to the tube to allow supplying gas while in the bore of the NMR. We used an analogous system to the one described before^[48,51]: hydrogenation pressure was 7 bar: pressure difference of 0.1 bar was used for pH₂ bubbling. We used a liquid nitrogen pH₂ generator^[47] to prepare 50% pH₂ hydrogen gas. The pH₂ gas line was flushed with N₂ for approximately 5 s at 5 bar to the atmosphere before connecting to the NMR tube to prevent hydrogenation. The NMR tube was cleaned with nitric acid (Chemsolute, art. 865, min 65% HNO₃), acetone (Chemsolute art. 2661, min 99.8%), and chloroform (Chemsolute, art 2476, min 99.9%) consequently before the experiment and dried with air.

After cleaning, the NMR tube was filled with 350 μL of PHIP-sample and connected to the gas line. We do not recommend using heavy wall high-pressure 5 mm NMR tubes for such experiments (e.g. 524-PV-7, Wilmad-LabGlass) because of the low internal volume of only 150 μL.

The NMR tube was placed into the NMR spectrometer, and allowed to reach temperature stabilization after 2-3 minutes: the temperature of the NMR probe was set to 330 K.

The pressure was built up in the system without flushing pH₂ through the sample that followed by 20 s of pH₂ bubbling through the solution at 7 bar. Then the pH₂ bubbling was stopped, and after 2 seconds of stabilization, the spin order transfer sequence (SOT) was executed.

Two-phase separation: 500 μL D₂O (Deutero GmbH) and 100 μL of 1 mol/L sodium hydroxide solution (Sigma Aldrich) were mixed in a standard 5 mm NMR tube. After hydrogenation with pH₂ and after the consecutive SOT, the sample was pneumatically shuttled to the NMR tube and shaken vigorously. The aqueous phase was on the bottom of the NMR tube and covered the active area of the NMR probe. This tube and an empty high-pressure NMR tube were exchanged, and the signal decay of the ¹³C signal was measured (**Figure 6e**).

3.2 PHIP NMR experimental details

Thermal experiments (Figure 6b1, 6c1) consisted of a 90° ¹H or ¹³C RF pulse and a free induction decay (FID) acquisition. Thermal spectra were recorded more than 10 minutes after hydrogenation. These spectra were used to measure integrals of ¹H and ¹³C at thermal equilibrium. Two integrals for 1-¹³C-EP-*d6* quantification were used: one for ¹H $I^{\text{th}}(\text{CHD})$ and one for ¹³C $I^{\text{th}}(^{13}\text{C})$. We integrated methylene hydrogen of ¹³C-EP-*d6* (CHD) as the methyl proton was buried under the other signals.

PASADENA experiment (Figure 6b1) consisted of a 45° ¹H RF pulse and a FID acquisition. Signal enhancement pro line ϵl was determined by dividing the absolute sum of four polarized lines in the ¹H PASADENA spectrum Il and dividing it by two integrals of methylene proton $I^{\text{th}}(\text{CHD})$: $\epsilon l = Il/2I^{\text{th}}(\text{CHD})$. The integral over the four polarized lines is the same for all within a few %. The lifetime of PASADENA polarization (**Figure 6b2**) was measured using a series of small flipping angle excitations: $[\varphi - \text{FID}]_n$ with $\varphi = 2.5^\circ$ and a repetition time TR = 4 s.

ESOTHERIC experiment (Figure 6c, S1). An ESOTHERIC^[16] pH₂ to ¹³C SOT sequence was used in the experiment ($\tau_1 = \tau_3 = 84$ ms, $\tau_2 = 36$ ms, total time = $2(\tau_1 + \tau_2 + \tau_3) = 408$ ms). The ¹³C-Signal enhancement ε is the ratio of ESOTHERIC integral $I^{\text{hyp}}(^{13}\text{C})$ and corresponding thermal integral $I^{\text{th}}(^{13}\text{C})$: $\varepsilon = I^{\text{HP}}(^{13}\text{C})/I^{\text{th}}(^{13}\text{C})$. We used an ESOTHERIC-L modification (Figure S1b) to obtain a longitudinal ¹³C-magnetization. This was useful to measure the lifetime of the ¹³C polarization (Figure 6c2) and to enable the cleavage of sidearm and two-phase separation outside of the magnet (Figure 6d) with subsequent signal measurement (Figure 6e). A series of ¹³C RF pulses with a small flipping angle of $\phi = 5^\circ$ and time interval TR = 4 s was used to measure the lifetime of the hyperpolarized ¹³C longitudinal magnetization in chloroform-d (Figure 6c2) and aqueous solution (Figure 6e2).

Polarization

¹³C-polarization is the product of signal enhancement ε and thermal polarization at given conditions: $P_{^{13}\text{C}}^{\text{HP}} = \varepsilon \cdot P_{^{13}\text{C}}^{\text{th}}$ with $P_{^{13}\text{C}}^{\text{th}}(9.4 \text{ T}, 330 \text{ K}) = 7.32 \cdot 10^{-6}$. ¹H-PASADENA or multiplet polarization is the product of average line enhancement εl , thermal ¹H polarization $P_{^1\text{H}}^{\text{th}}$ times two: $mP_{^1\text{H}}^{\text{HP}} = 2 \cdot \varepsilon l \cdot P_{^1\text{H}}^{\text{th}}$ with $P_{^1\text{H}}^{\text{th}}(9.4 \text{ T}, 330 \text{ K}) = 2.91 \cdot 10^{-5}$. We include a factor of 2 here because multiplet polarization is a two-spin state, and after 45° RF pulse, both spins have the same signal. If one instead uses e.g. selective-90° RF pulse, then one proton would have a double signal and the absolute amplitude of each line, in this case, will be equal to 100% of net polarization (see e.g. ref ^[48]). The reported enhancements values are the best within three repetitions of the experiment.

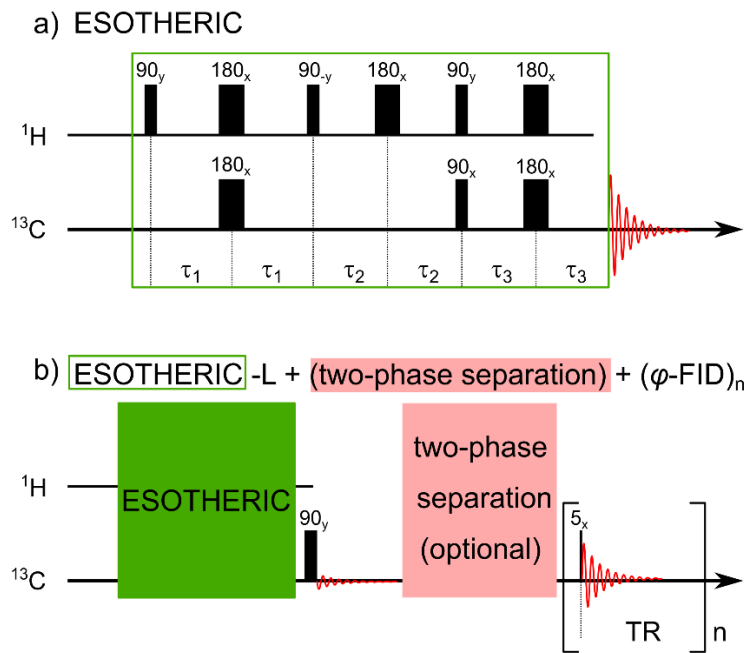


Figure S1. ESOTHERIC (a) and ESOTHERIC-L (b) SOT sequences with optional two-phase separation stage. ESOTHERIC prepares transversal ¹³C polarization (a). An additional 90° pulse is required to convert it to longitudinal polarization (b). Longitudinal polarization can be manipulated, and magnetic field inhomogeneity does not destroy it. We measured the lifetime of polarization using a series of small flipping angle excitations: $[\varphi - \text{FID}]_n$ with $\varphi = 5^\circ$ and repetition time TR = 4 s. Then the exponentially decaying signal was fitted with mono exponentially decaying function: $f(n) = A \cdot \exp\left[-n \frac{\text{TR}}{T_{\text{HP}}^{\varphi, \text{TR}}}\right]$. The life of hyperpolarization then is equal to $T_{\text{HP}} = \left(\frac{1}{T_{\text{HP}}^{\varphi, \text{TR}}} + \frac{\ln[\cos(\varphi)]}{\text{TR}}\right)^{-1}$. This is simple to derive from equality $f(n) = A \cdot \exp\left[-n \frac{\text{TR}}{T_{\text{HP}}^{\varphi, \text{TR}}}\right] = A \cdot \exp\left[-n \frac{\text{TR}}{T_{\text{HP}}}(\varphi)\right]$.

4. Spectroscopic data

4.1 Vinyloxy silanes

4.1.1 Vinyloxy silanes: dimethylisopropyl(vinyloxy)silane (4b)

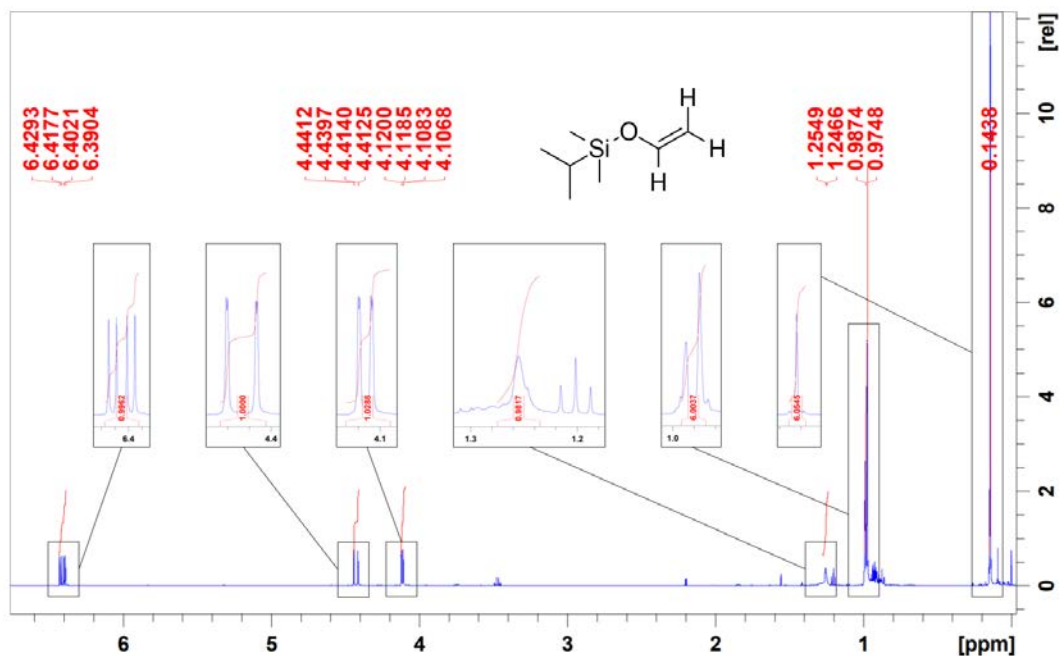


Figure S2. ¹H NMR spectrum of 10 μ L dimethylisopropyl(vinyloxy)silane in 500 μ L chloroform-d.

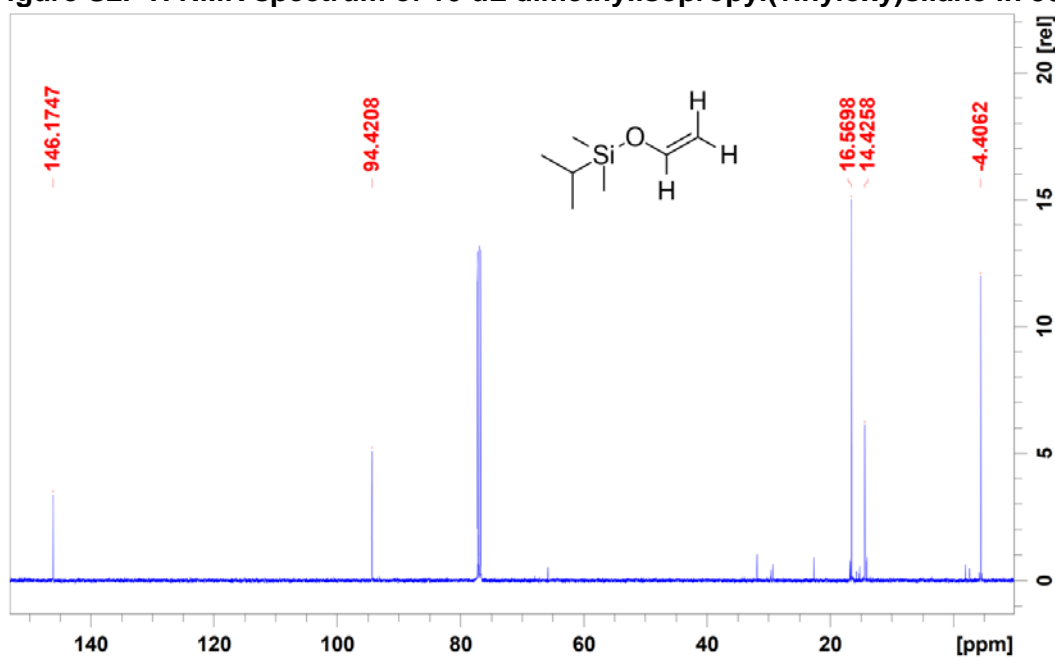


Figure S3. ¹³C NMR spectrum of 10 μ L dimethylisopropyl(vinyloxy)silane in 500 μ L chloroform-d.

4.1.2 Vinyloxy silanes: dimethylisopropyl(vinyloxy)silane-d₃ (4c)

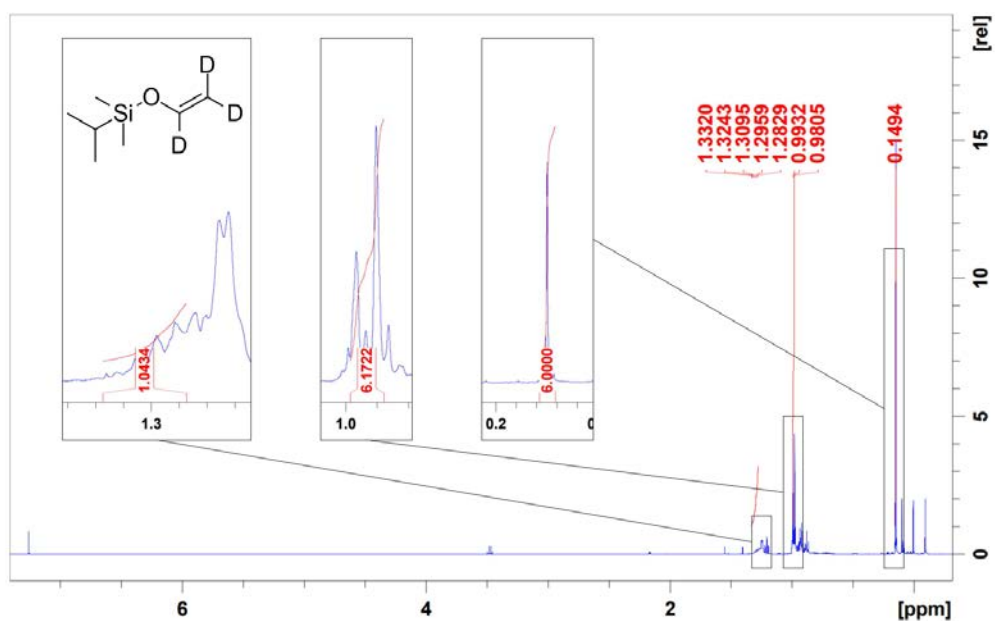


Figure S4. ¹H NMR spectrum of 10 uL D₃-dimethylisopropyl(vinyloxy)silane in 500 uL chloroform-*d*.

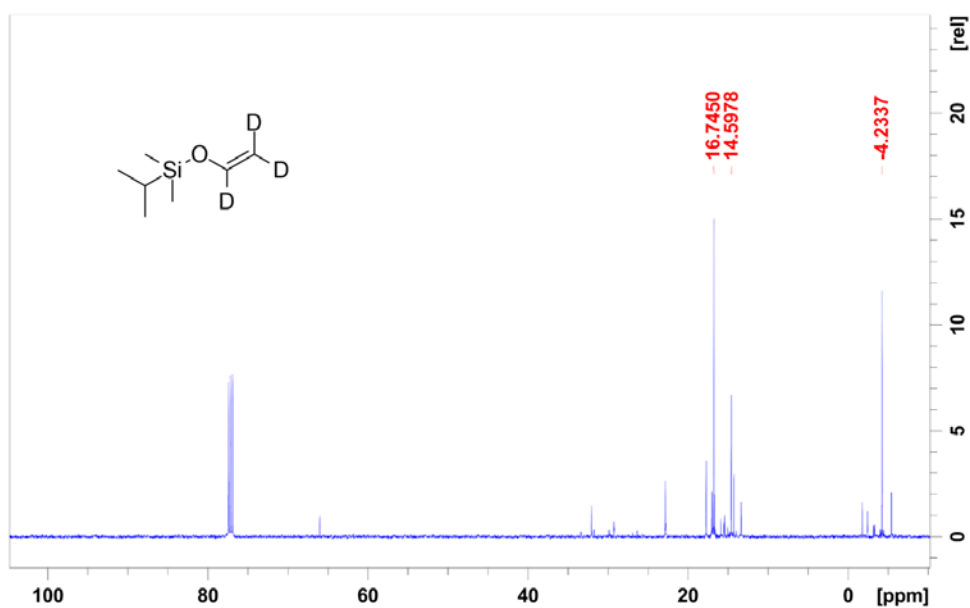


Figure S5. ¹³C NMR spectrum of 10 uL dimethylisopropyl(vinyloxy)silane-*d*₃ in 500 uL chloroform-*d*.

4.2 Vinyl pyruvates

4.2.1 Spectra of vinyl pyruvate (2a)

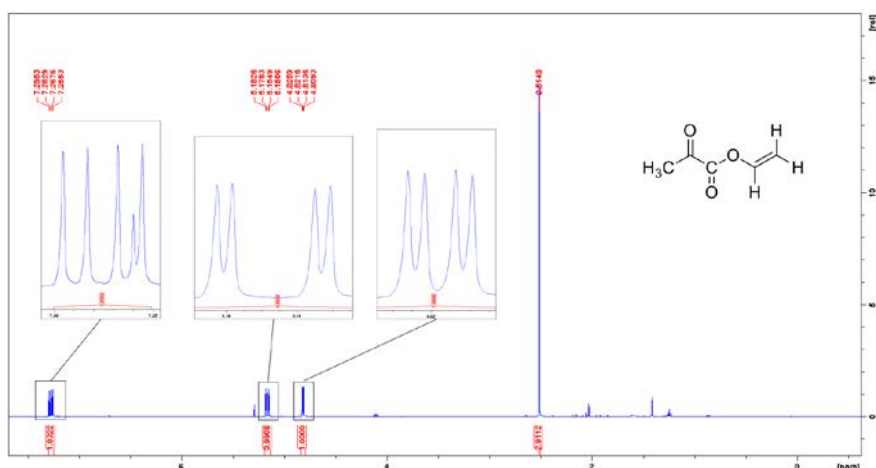


Figure S6. ^1H NMR spectrum of 10 μL VP in 500 μL chloroform-d.

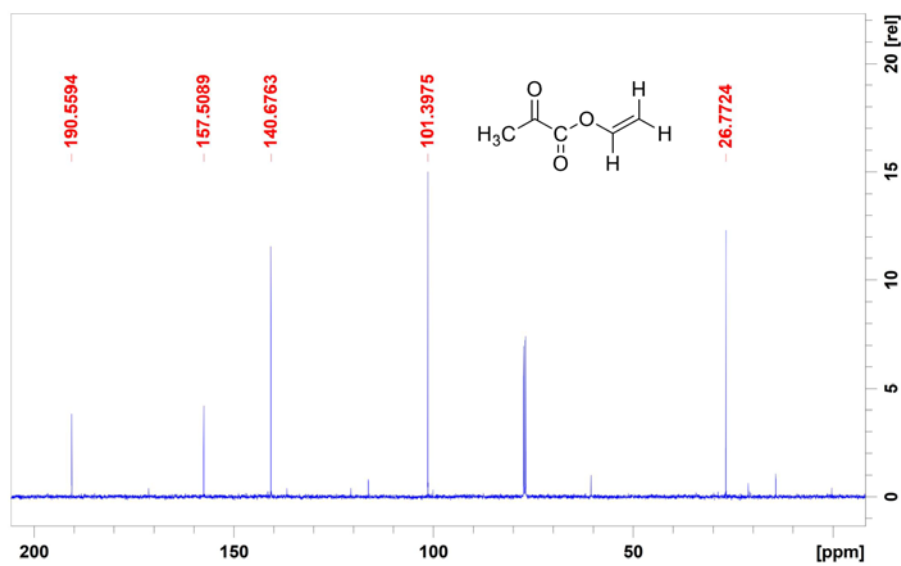


Figure S7. ^{13}C NMR spectrum of 10 μL in 500 μL chloroform-d.

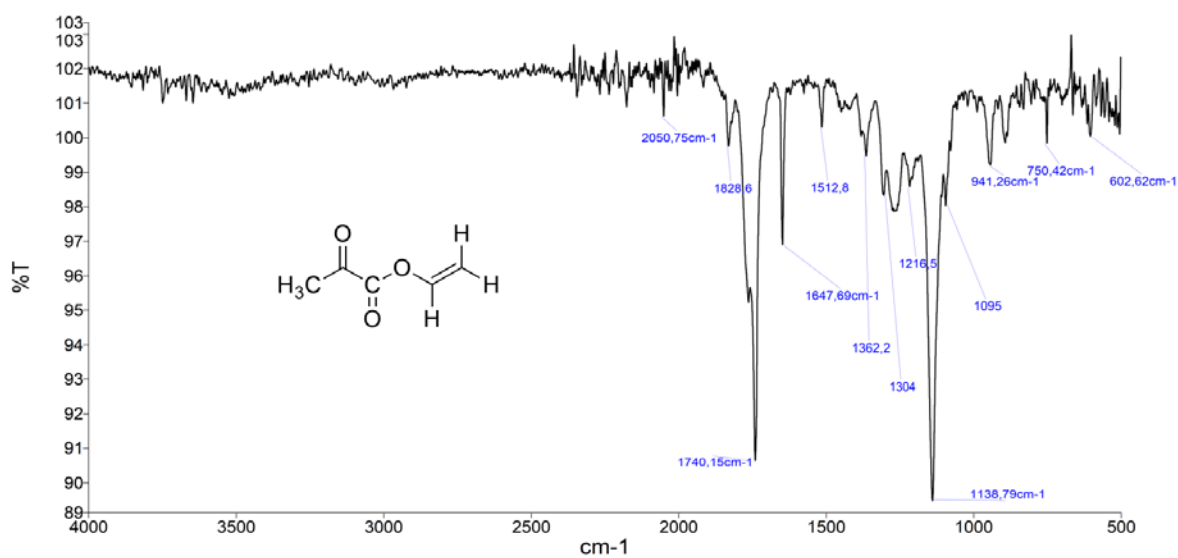


Figure S8. IR spectrum of vinyl pyruvate (2a).

4.2.1 Spectra of 1-¹³C-vinyl pyruvate (2b)

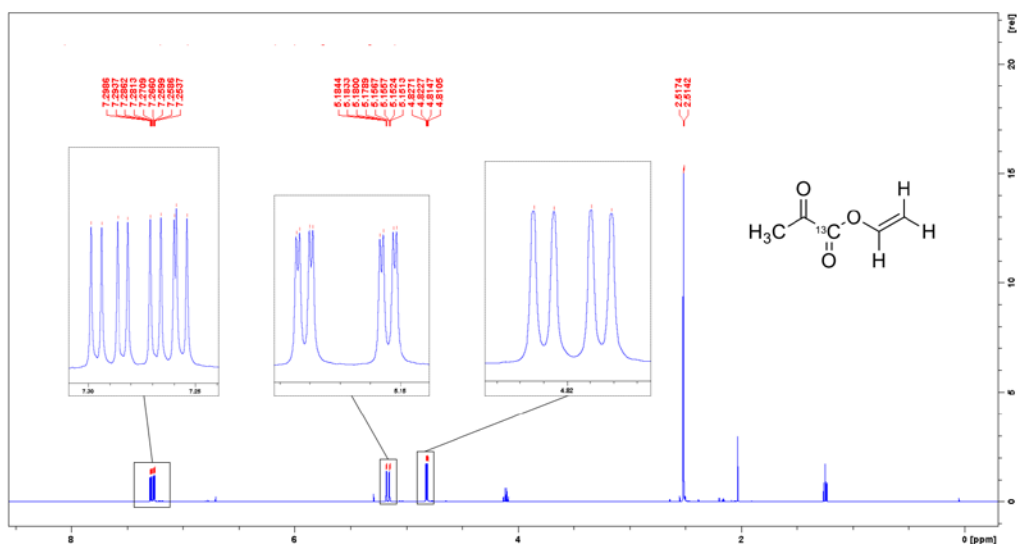


Figure S9. ¹H NMR spectrum of 10 μ L 1-¹³C-VP in 500 μ L chloroform-*d*.

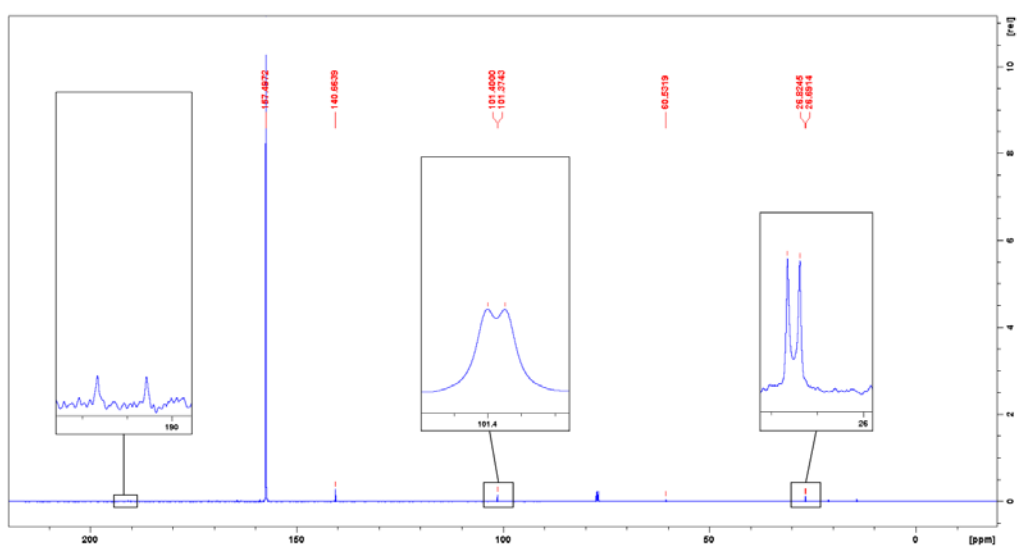


Figure S10. ¹³C NMR spectrum of 10 μ L 1-¹³C-VP in 500 μ L chloroform-*d*.

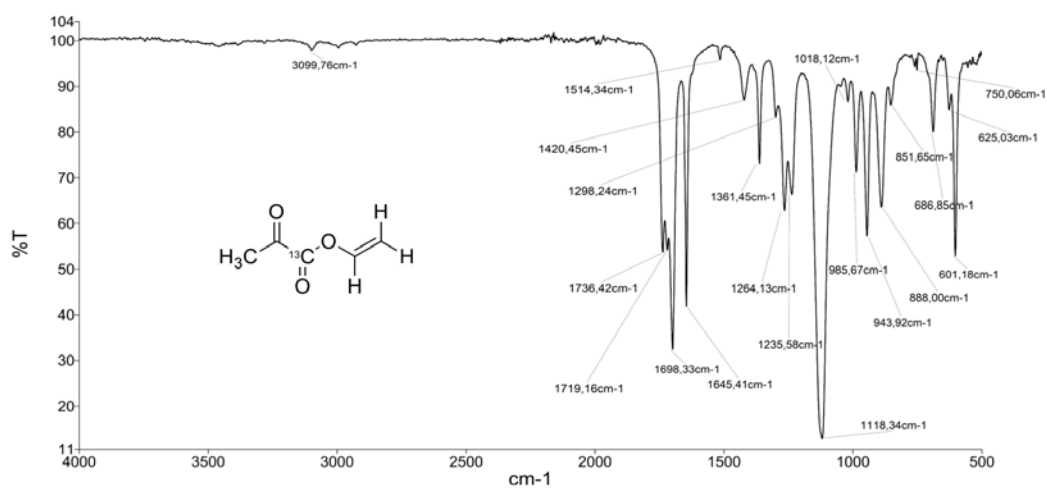


Figure S11. IR spectrum of 1-¹³C-VP.

4.2.3 Spectra of vinyl pyruvate-*d*3 (2c)

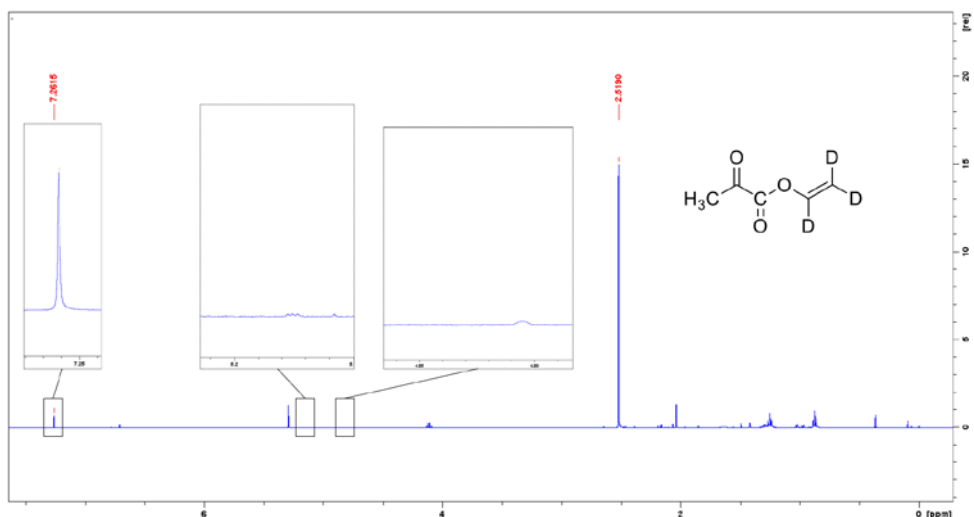


Figure S12. ¹H NMR spectrum of 10 uL VP-*d*3 in 500 uL chloroform-*d*.

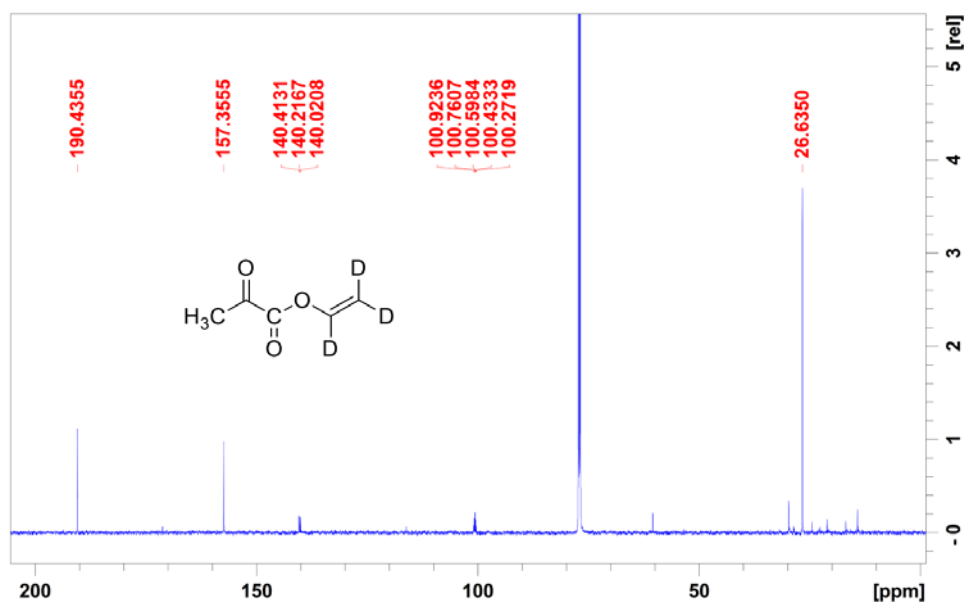


Figure S13. ¹³C NMR spectrum of 10 uL VP-*d*3 in 500 uL chloroform-*d*.

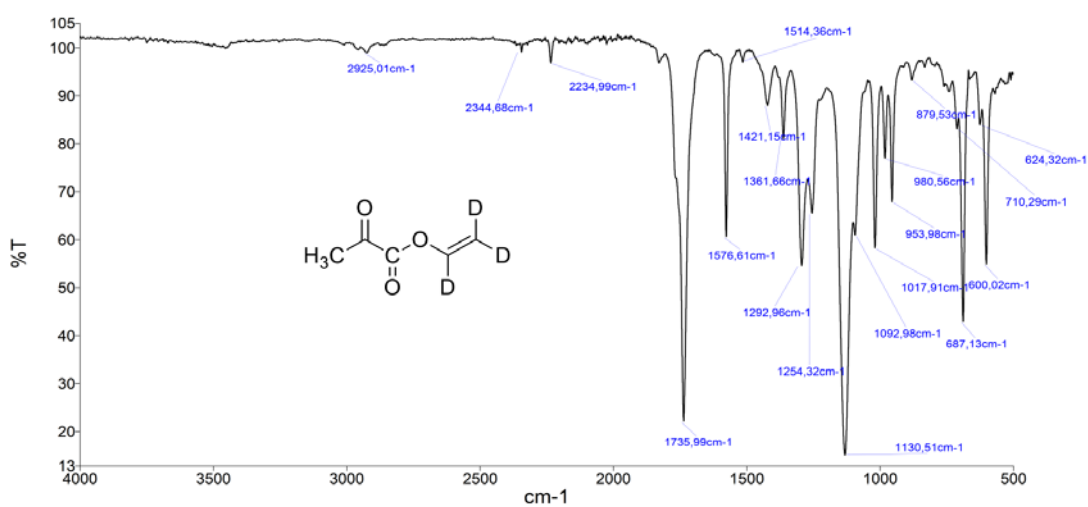


Figure S14. IR spectrum of VP-*d*3.

4.2.4 Spectra of 1-¹³C-pyruvate-d3 (2d)

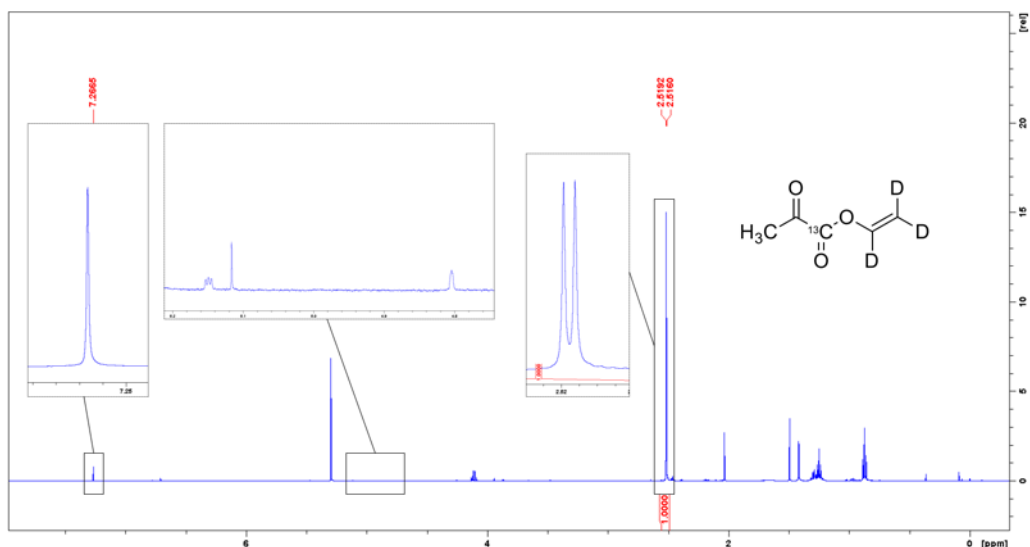


Figure S15. ¹H NMR spectrum of 10 μL 1-¹³C-VP-d₃ in 500 μL chloroform-d.

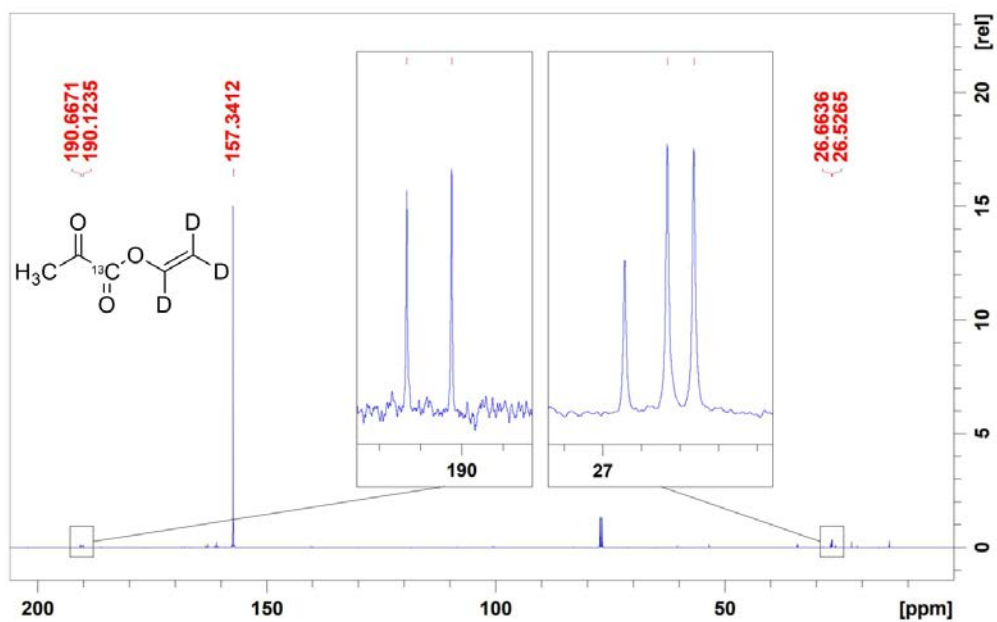


Figure S16. ¹³C NMR spectrum of 10 μL 1-¹³C-VP-d₃ in 500 μL chloroform-d.

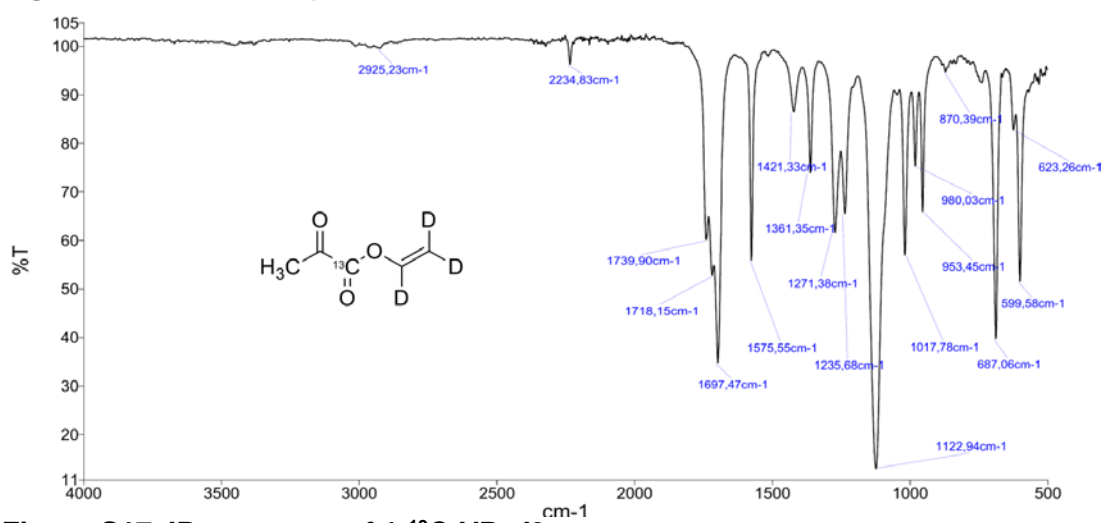


Figure S17. IR spectrum of 1-¹³C-VP-d₃.

4.2.5 Spectra of 1-¹³C-vinyl pyruvate-*d*6 (2e)

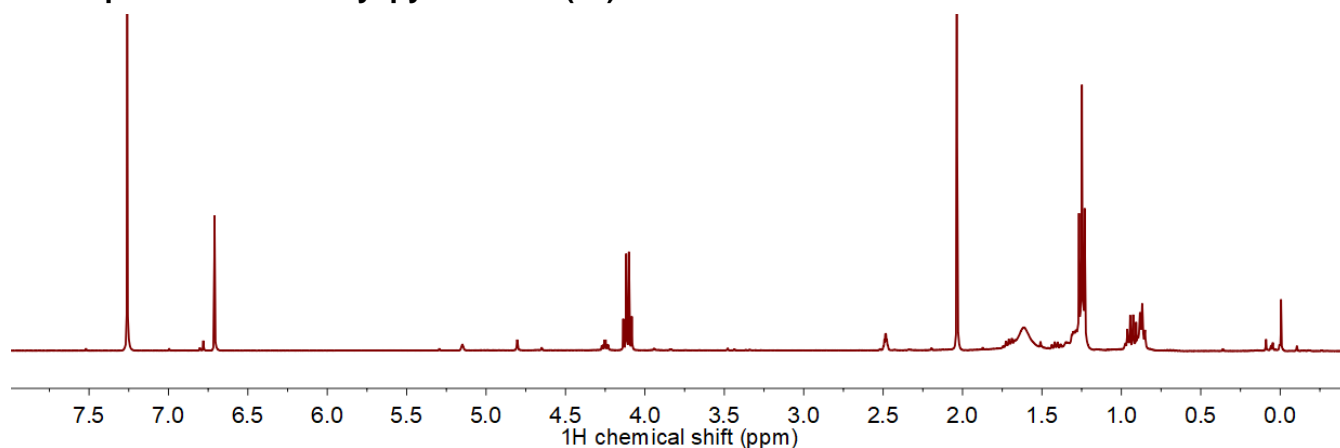


Figure S18. ¹H NMR spectrum of 10 uL 1-¹³C-VP-*d*6 in 600 uL chloroform-*d*. Acquisition parameters: receiver gain is 101, number of scans is 64. No 1-¹³C-VP-*d*6 signals are visible. Main impurity is ethyl acetate.

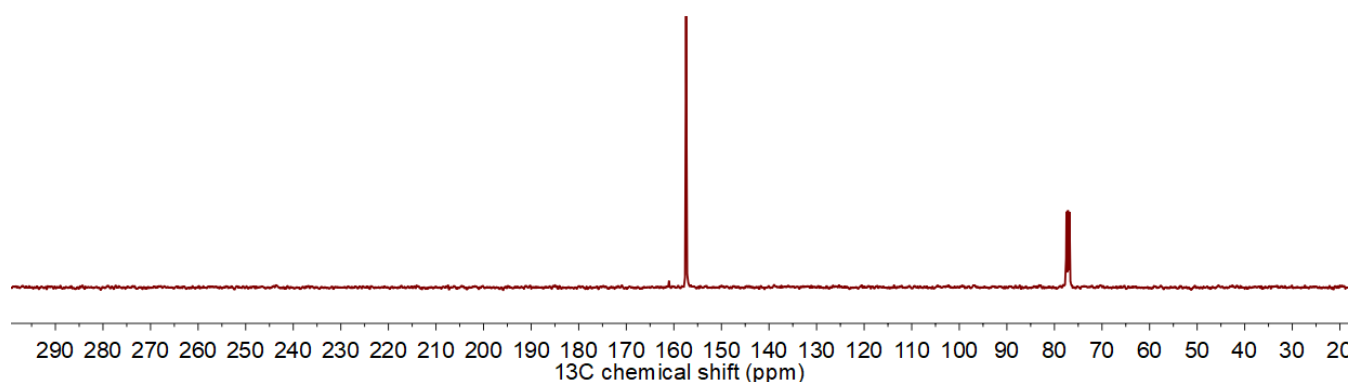


Figure S19. ¹³C NMR spectrum of 10 uL 1-¹³C-VP-*d*6 in 600 uL chloroform-*d*. Acquisition parameters: receiver gain is 101, number of scans is 64. T1 relaxation time for 1-¹³C-VP-*d*6 (157.44 ppm) was measured with t1ir with d1+aq = 351 s to be 43 s. Chemical shifts are calibrated to ¹³C-chloroform-*d* signal at 77.16 ppm (T1 73 s).

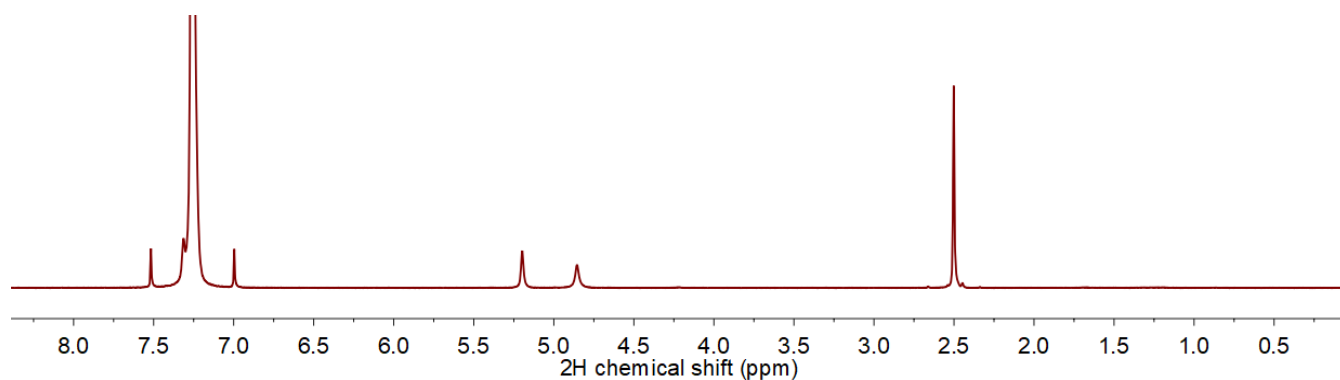


Figure S20. ²H NMR spectrum of 10 uL 1-¹³C-VP-*d*6 in 600 uL chloroform-*d*. Acquisition parameters: receiver gain is 36, number of scans is 64. T1 relaxation time for 1-¹³C-VP-*d*6 (157.44 ppm) was measured with t1ir with d1+aq = 10 s to be 0.27 s for CD₂^a (5.2 ppm), <0.1s for CD₂^b (4.2 ppm) and 1.4 s for CD₃ (2.5 ppm). Chemical shifts are calibrated to chloroform-*d* at 7.26 ppm, (T1 1.3 s).

4.3 NMR spectra of 1-¹³C-EP-d6 (hydrogenation product of 2e)

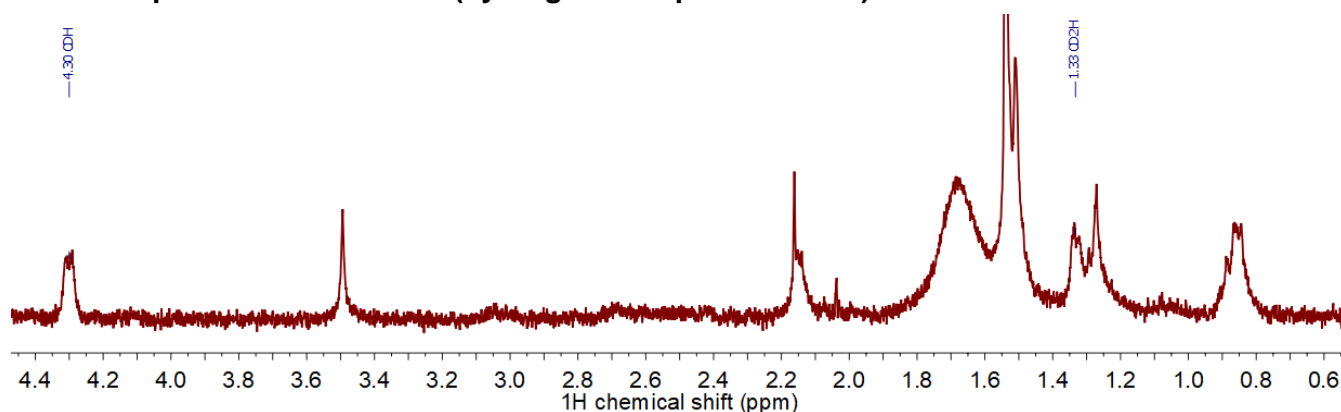


Figure S21. ¹H NMR spectrum of hydrogenated 2 mM 1-¹³C-VP-d6 to 1-¹³C-EP-d6 chloroform-d. Chemical shifts of two peaks of H₂ nascent protons are indicated. We mentioned in the main text that the methyl proton (CD₂H, 1.33 ppm) was not integrated to measure signal enhancement. Here we show that it was covered with other signals, however, the methyl proton (CDH, 4.30 ppm) is isolated and perfectly suited for integration. The spectrum was measured about 10 minutes after hydrogenation of 1-¹³C-VP-d6. Chemical shifts are calibrated with respect to chloroform-*h* at 7.26 ppm.

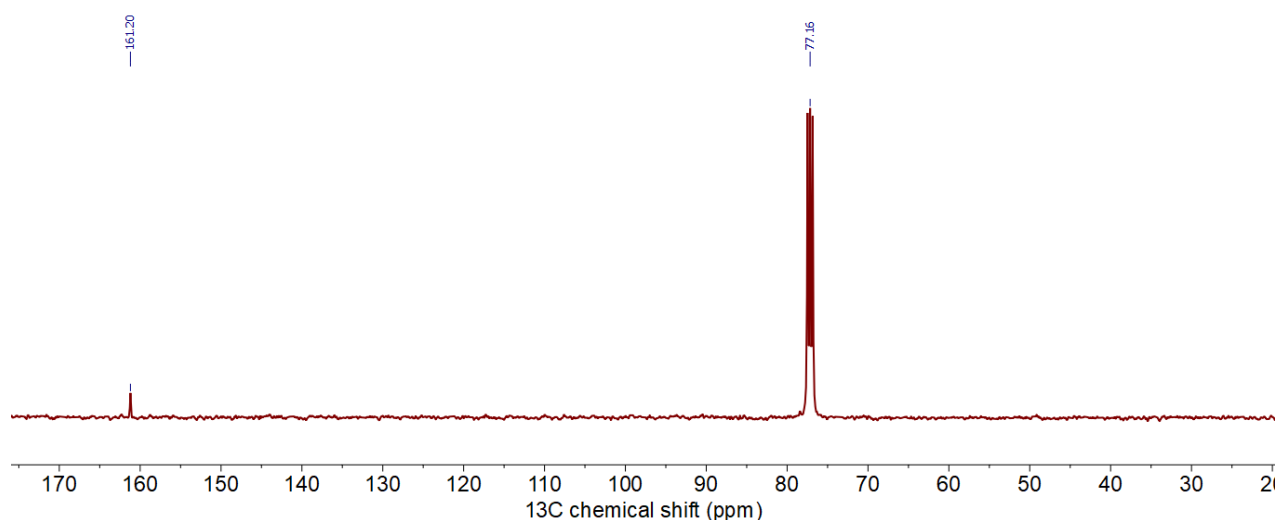


Figure S22. ¹³C NMR spectrum of hydrogenated 2 mM 1-¹³C-VP-d6 to 1-¹³C-EP-d6 chloroform-d. Acquisition parameters: receiver gain is 101, number of scans is 32. Chemical shifts are calibrated to ¹³C-chloroform-*d* signal at 77.16 ppm.

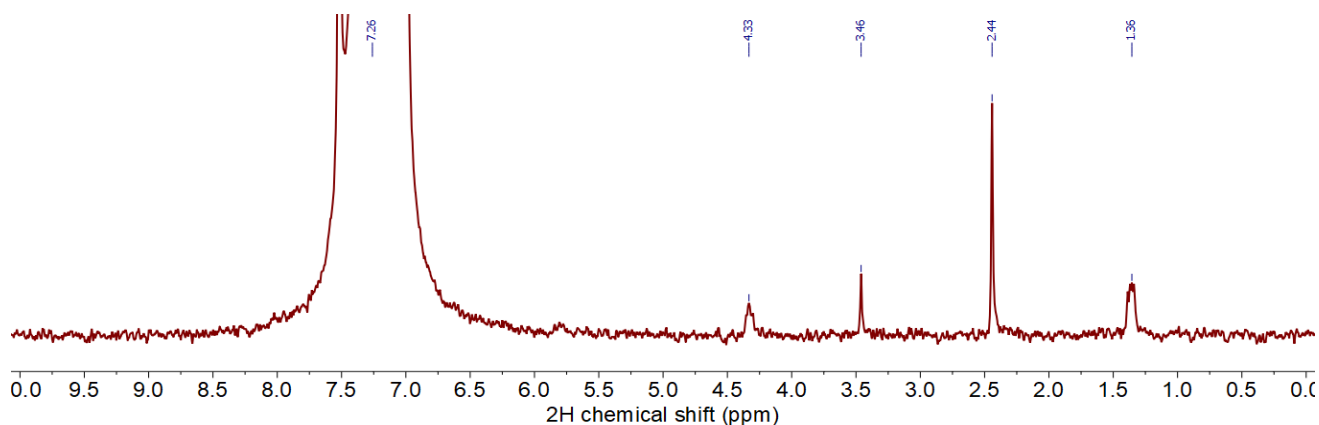


Figure S23. ²H NMR spectrum of hydrogenated 2 mM 1-¹³C-VP-d6 to 1-¹³C-EP-d6 chloroform-d. Acquisition parameters: receiver gain is 101, number of scans is 512. Chemical shifts are calibrated to chloroform-*d* at 7.26 ppm.